

UNIVERSITY OF OKLAHOMA

GRADUATE COLLEGE

AN EXPERIMENTAL STUDY OF THE WELLBORE CEMENT BONDING AND  
SHEAR STRESS

A THESIS

SUBMITTED TO THE GRADUATE FACULTY

in partial fulfillment of the requirements for the

Degree of

MASTER OF SCIENCE

By

MI CHIN YI

Norman, Oklahoma

2019

AN EXPERIMENTAL STUDY OF THE WELLBORE CEMENT BONDING AND  
SHEAR STRESS

A THESIS APPROVED FOR THE  
MEWBOURNE SCHOOL OF PETROLEUM AND GEOLOGICAL ENGINEERING

BY

Dr. Catalin Teodoriu, Chair

Dr. Saeed Salehi

Dr. Mashhad Fahs

© Copyright by MI CHIN YI 2019

All Rights Reserved.

## **Acknowledgement**

I would like thank my research advisor Dr. Catalin Teodoriu for his all efforts, guidance, and patience throughout my whole academic journey at the University of Oklahoma. Even when I had a hard time due to numerous things, he has been such a supportive and humorous advisor. Therefore I couldn't give up.

To Dr. Salehi, for his outstanding lectures in classes such as Human Factors in Drilling Operation and his numerous publications that I learned a lot for my research work. To Dr. Fahs, as the other valuable committee member of this thesis.

I also would like to thank The Mewbourne School of Petroleum and Geological Engineering at the University of Oklahoma for any support that I have been given.

Lastly, thank my family, dear friends, whoever supported me mentally or physically for the entire school life as well as colleagues at the Well Integrity Lab for their collaborations and helps.

Wherever I will be, I will always be excited to hear "Boomer Sooner".

MI CHIN YI, Class of 2018

## Table of Contents

Acknowledgements.....	iv
Table of Contents.....	v
List of Tables.....	vii
List of Figures.....	viii
Abstract.....	x
1. Introduction.....	1
1.1. Motivation.....	1
1.2. Literature Review.....	4
1.3. Objectives.....	18
2. Wellbore Integrity and Wellbore Cement .....	20
2.1. Life of Well, Cement, and Wellbore Integrity .....	20
2.2. Wellbore Cementing Fundamentals.....	23
2.3. Wellbore Cement Classification.....	25
2.4. Cement Shear Bonding Strength Mechanism.....	30
2.4.1 Intermolecular Bonding.....	30
2.4.2 Chemical Bonding.....	30
2.4.3 Mechanical Bonding.....	30
2.5. Thesis Idea.....	31
2.5.1 Shear Failure Mechanisms.....	33
3. Experiment.....	35
3.1. Cement Mixing.....	36
3.2. Cement Curing.....	37
3.3. Cement Sample Geometry.....	40
3.4. Mechanical Strength Test.....	45
3.4.1. Pure Cement Shear Stress.....	47
3.4.2. Bonding Stress.....	49
3.4.3. UCS.....	50
4. Acquire Data and Analysis.....	52
4.1. Correlations.....	52
4.2. Calculation Method.....	53
4.3. Result Data.....	55
4.3.1 Non-thermal Effect Data.....	56
4.3.2 Thermal Effect Data.....	58
5. Discussion .....	59
5.1. Shear Stress .....	59
5.2. Bonding Stress.....	63

5.3. Unconfined Compression Stress (UCS).....	65
5.4. Test Result Comparison.....	68
5.5. Comparison Between 3 days Non-thermal and Thermal Effect Result.....	72
5.6. Correlation of UCS Vs. Shear / UCS Vs. Bonding.....	73
6. Conclusions and Recommendation.....	76
References.....	80

## **List of Tables**

- Table 1- Portland Cement Class (Nelson and Gulliot 2006)
- Table 2 - Various Additives, Purpose of Use, and Main Function (Nelson 1990)
- Table 3- Geometry of Shear and Bonding Cells
- Table 4- Cement and Shear Cell Contacting Area
- Table 5- Cement and Bonding Cell Contacting Area
- Table 6- Bonding Stress Experiment Results
- Table 7- Shear Stress Experiment Results
- Table 8- Unconfined Compressive Strength Test Results
- Table 9- Comparison Between 3day Curing Room Temperature and High Temperature Bonding stress
- Table 10- Comparison Between 3day Curing Room Temperature and High Temperature Shear Stress
- Table 11- The Average Values from All Shear Test with Curing Days
- Table 12- The Average Values from All Bonding Test with Curing Days
- Table 13- The Average Values from All UCS Test with Curing Days
- Table 14- Comparison of literature values with obtained data

## List of Figures

- Figure 1- Energy Consumption by Sector (left), Energy Consumption by Fuel (right), (EIA 2017)
- Figure 2- Drilled Wells and Completed Trend (Rystad Energy 2018)
- Figure 3- Schematic of Wellbore Cementing (Checkai et al, 2013)
- Figure 4- Example of Possible Leakage Path for CO<sub>2</sub> in a Cased Wellbore (Celia et al, 2004)
- Figure 5- Failure Sequence During Testing (Kosinowski et al, 2012)
- Figure 6- Types of Mechanical Cement Failure a) Radial Crack b) De-bonding c) Shear Failure (Wehling 2008)
- Figure 7- Redrawn Double Shear Push Bond Test Setup (Haddad et al, 2013)
- Figure 8- Shear Bonding Test and Hydraulic Test Between Pipe and Cement setup (Evans and Carter, 1962)
- Figure 9- Bonding difference using Slag Cement and Conventional Cement (Silva et al, 1997)
- Figure 10- API Class H Portland Cement Sample (right) and fly ash geopolymer sample (left) prepare for shear bond testing. (Salehi et al, 2017)
- Figure 11- Casing Schematics (Rigzone)
- Figure 12- Wellbore and Cement (Drilling Course, 2015)
- Figure 13- Oilwell Cement from Surface to Wellbore
- Figure 14- Placement Techniques for Primary Cement (Smith 1974)
- Figure 15- Portland Cement Production Workflow (Ichim 2015)
- Figure 16- Change of Wellbore Cementing Phase
- Figure 17- Change of Wellbore Cementing Phase
- Figure 18- Cement Shear (A) and Bonding Stress (B) near Coupling
- Figure 19. Transition From Brittle to Ductile. (Maurer 1965)
- Figure 20- Shear (Left), Bonding (Center), UCS Cubes(Right) Molds
- Figure 21- Experimental Samples Curing in Room Temperature Water
- Figure 22- Hot Tub (Left) for High Temperature Curing and Samples (Right)
- Figure 23- Bonding (Left), Shear(Center), UCS cubes(Right)Samples after Testing

Figure 24- Shear (Left) Cell Cut-Off Diagram, Bonding (Right) Cell Cut-Off Diagram

Figure 25- Bonding Stress Diagram Showing Displacement and Length

Figure 26- Shear Stress Diagram Showing Length

Figure 27- UCS Cubes Length and Width

Figure 28- Hydraulic Press (Central Machinery)

Figure 29- DASyLab

Figure 30- Shear Stress Setup (Left), Shear Mold Front View (Center), Inside View (Right)

Figure 31- Bonding Stress Setup (Left), Bonding Mold Front View (Center), Inside View (Right)

Figure 32- CM-2500 Compression Testing Machine (Romanowski et al, 2017)

Figure 33- Proposed Correlation of Force Vs. Gauge

Figure 34- Example of the Maximum Force Before Failure: 3-day bonding test

Figure 35- Shear Stress Evolution with Curing Days

Figure 36- Shear Stress Samples 1day Curing (Left) and 7-day Curing (Right)

Figure 37 - Bonding Stress Evolution with Curing Days

Figure 38 - Bonding Stress 1day Curing (Left) and 7-day Curing (Right)

Figure 39- UCS Evolution with Curing Days

Figure 40- Comparison of UCS Cubes After Test. 1-day Curing (Above), 7-day Curing (Below)

Figure 41- Plot Comparison of Shear, Bonding, and UCS with Curing Days

Figure 42- Unconfined Compressive Strength Evolution with Time at 25C (Ichim, 2018)

Figure 43- Relative Shear and Bonding Stress to UCS with Curing Time

Figure 44- 3-day curing Thermal effected and Non-thermal effected Shear and Bonding Stress Comparison 1

Figure 45- 3-day curing Thermal effected and Non-thermal effected Shear and Bonding Stress Comparison 2

Figure 46. Class H Cement Shear and UCS Correlation

Figure 47. Class H Cement Bonding and UCS Correlation

## **Abstract**

Well Integrity is considered one of the most important topics in petroleum industries. A failure of well integrity causes many undesirable consequences such as loss of human lives, loss of drilling equipment or production facilities, loss of hydrocarbon reserves, and pollution. (Santos 2017)

A successful cementing is a major contribution that leads wellbore integrity to be secured. Because cementing is a complex job that is involved with many variable factors, it is important to understand wellbore cementing behaviors in various environments and factors that affect to it.

Wellbore integrity issues should be observed not only during a well is producing hydrocarbons but from the well construction phase to the well abandonment. Likewise, cementing should stay healthy throughout the entire well life. As more wells have been drilled and abandoned over the years, more researchers have started to pay attention to well integrity issues. With this trend, efforts to understand cement behaviors have been increased. As mentioned earlier, cementing is not as simple as it sounds due to various factors involved to its chemistry, mechanics and many others. Therefore, factors that cause cement failure can be diverse.

Plenty of studies have focused on cement compressive and tensional strength to investigate cement mechanics affected by forces. Some researchers also have investigated bonding stresses of contact between cement and casings. These studies

have found de-bonding at contacts between cement and casings or casing and formation to explain wellbore integrity failure. However, field data show that there is no correlation between de-bonding theory and the casing movement. If that is the case, the major assumption is made that cementing hardware such as centralizer or thread collars do not restrict casing axial movement, and the regional stresses caused at near couplings could be huge influences to wellbore failures.

With this hypothesis, this master's thesis introduced a new method to investigate special cement properties (pure cement shear, bonding, and Unconfined Compressive Strength) caused at near casing as well as coupling installed area by replicating the interaction between the casing coupling and cement in a lab size.

## **1. Introduction**

### 1.1 Motivation

Current energy industry has been going through a transition phase from traditional energy to renewable energy due to a drastic advent of advanced technologies, increased attention to environmental issues, and also political issues. The importance of seeking newer and cleaner energy has been discussed over the years. Even though securing clean and renewable energy has been suggested as a critical agenda for a future energy industry, analysis from various researches show that oil and gas will still be demanding for a few more decades.

Recently, EIA (Energy Information Administration) released a prediction showing that the total US production would increase by 31% from 2017 through 2050 in their annual report. (EIA, 2018)

The increase in energy production is supported by the graphs in Figure1. The left chart shows the energy consumption trend by sector. Based on the historical trends, the electric power will still be the most energy-consumed and industrial sector will keep increasing. To sum up, the entire energy consumption from all sectors will be higher than the history and it will end up resulting higher energy demanding. The right chart shows the prediction of energy consumption by fuel. Even though renewable energy consumption will be in a trend of increase towards 2050, the

prediction says that the sum of petroleum and natural gas consumption will be dominant. (EIA 2018)

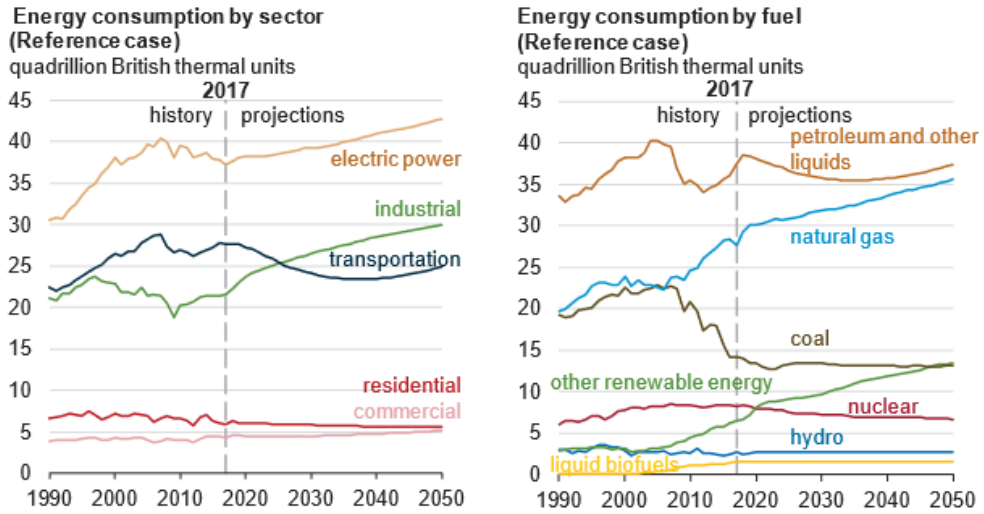


**Figure1. Energy Consumption by Sector (left), Energy Consumption by Fuel (right), (EIA, 2017)**

As oil and gas production is increasing as research predictions, well construction and abandon well is going to increase accordingly. More focused on a short-term prediction, Rystad Energy recently has released an outlook for worldwide drilling and well service market. According to Rystad Energy, the oil industry is expected to drill and complete 72,000 wells growth world in 2019, which is 3% increasing compare to 2018 (Rystad Energy, 2018). The Figure2 shows that drilling and completion activity has grown approximately 30%, and the activity growth to be an average annual rate of 4% towards 2021.

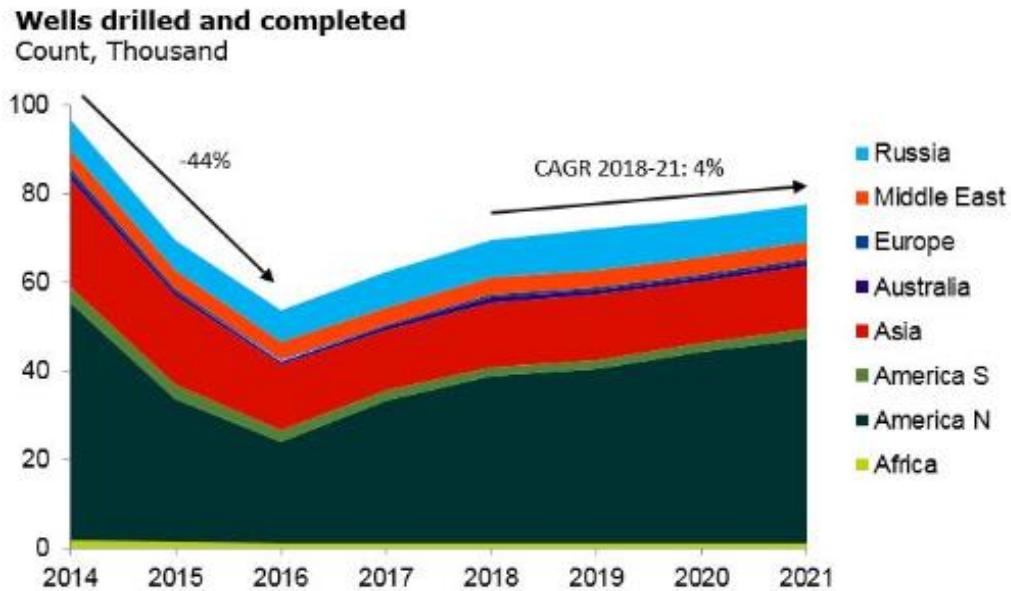


**Figure2. Drilled Wells and Completed Trend (Rystad Energy, 2018)**

Since drilling wells and completion activity has been recognized as inevitable jobs for extracting hydrocarbon as long as the world demands energy from oil and gas industry, many researchers and people from the industry had started to be interested in well integrity issues. According to Ichim (2016), approximately 22,000 technical literatures that deal with a topic of well integrity has been published in OnePetro, and almost 60% of these publications has been published in the last decades. It obviously shows an increases interest in specific topic of well integrity in recent years. Cement properties, which is the objective in this thesis, are a crucial part of the entire well life in terms of securing wellbore integrity. Alber and Ehringhausen

(2017) stated that a successful cementing job is known as one of the most important jobs in achieving long term well integrity.

In shorts, not only during the well construction phase, cementing integrity preservation during completion, stimulation, production, and even at a phase of well abandonment is critical for an oil and gas industry in terms of long term economic, productivity, and safety perspectives. (Reddy et al, 2007)

## 1.2 Literature review

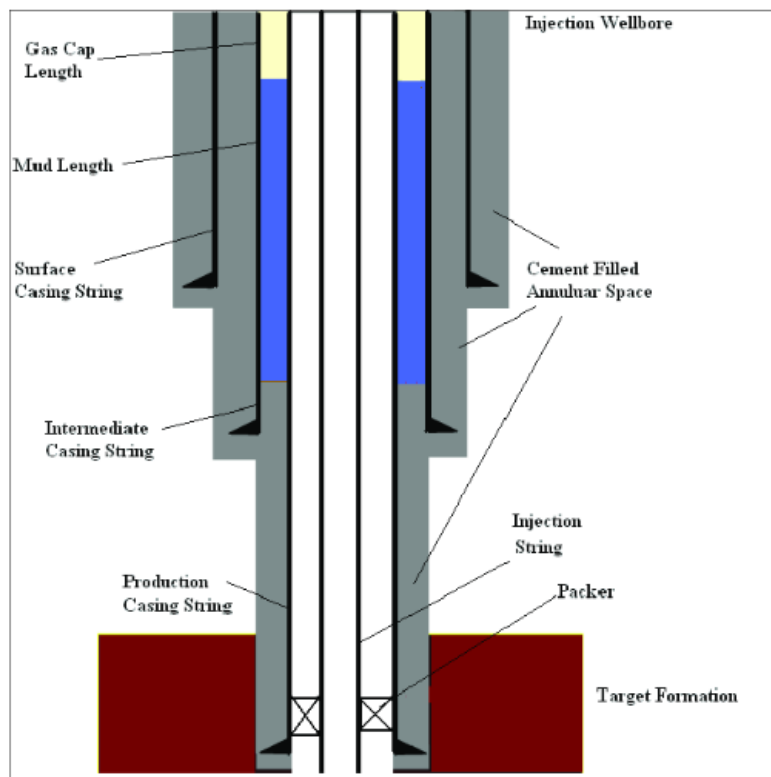
According to API (American Petroleum Institute), proper cement and cementing practices are an integral part of ensuring successful well integrity. The API also states that complete displacement of drilling fluid by cement and good bonding of the cement interfaces between the drilled hole and the casing immediately above the hydrocarbon formation are key parts of well integrity and seal integrity. (API, 2009)

Therefore, it is important that proper cement design, the slurry, its placement and ultimate objectives of the operation should be understood and agreed by all parties involved that is not only limited to drilling organization but also reservoir, geology, and completions. (Benge 2014)

Wellbore cementing is a process of placing cement in the annulus space between the well casing and the surrounding geological formation to provide zonal isolation

(ShahrUAR 2011), or between two strings of casing. The main objectives of well cementing are (Joshi and Lohita 1997):

- Providing axial and collapse support to the casing,
- Protecting well casing from corrosion,
- Reducing the risk of ground water contamination by oil, gas, or saltwater,
- Preventing crossflow (exchange of gas or fluids among different geological formation).



0 Schematic of Leaky Wellbore with Intermediate Annular Space Occupied by Mud (blue) and a Gas Cap (yellow).

**Figure3. Schematic of Wellbore Cementing (Checkai et al, 2013)**

Figure3 shows a brief schematic of wellbore cementing and its location around the wellbore. (Checkai et al, 2013)

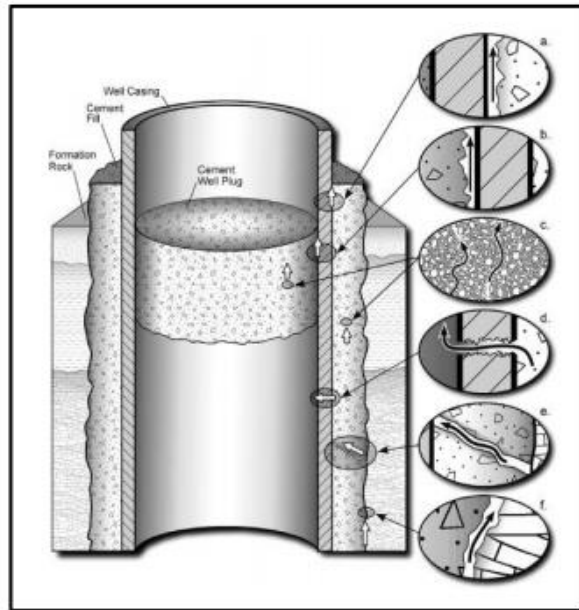


**Figure4. Example of Possible Leakage Path for CO<sub>2</sub> in a Cased Wellbore (Celia et al, 2004)**

In order to prevent cementing integrity failures, securing successful cement sheath is vital through the entire well life. Unhealthy cement sheath would cause improper fluid migration between wellbore and the formation, and it would end up causing negative effects on well integrity. Especially, gas migration can be considered as a major problem of possible leakage in cementing as shown in Figure4. (Celia et al, 2004) It shows a few examples of possible leakage path for CO<sub>2</sub> in cased wellbore. However, it is impossible to expect the wellbore cement would stay static and stable from the initial cementing stage to the end of the well life. In other words, we can

anticipate that cement degradations would most likely to happen under the heterogeneous formation conditions and from influences employed by other than geological variations. Since the geological variation and behavior of dynamic fluids in reservoir tend to be hard to predict due to their unexpected nature, investigation in mechanical influences while drilling and completion operations could be valuable in order to prevent cement failure.

Here, any mechanical influences in drilling, production, or completion operational phases could be from drill strings, casings, surface hardware or any other wellbore hardware.

Even though wellbore cement has been designed as best as it can be considering all factors that would affect to it, the placed cement into the wellbore most likely would face degradation at some point during the well life.

Understanding degradation of cement is extremely crucial to lead the whole cement system to a success. Failure of the cementing sheath would directly related to wellbore integrity issues and it could cause any kind of harm in aspects of environment, economics, human health, and human life.

Sometimes unsuccessful cementing job causes significant risk as it is proved at the Macondo incident which was happened in 2010 in the Gulf of Mexico. This tragedy is an example of the result that improper cementing job can cause a well control problem, which leads to the major incident. (Graham et al, 2011)

Vignes and Tønning (2008) stated that degradation in cement are usually caused due to temperature, mechanical and chemical influence, and corrosion. Among these effects, various mechanical effects on settled cement or cement mechanics have been studied by many researchers from various fields that is not only limited to oil and gas industry.

When it comes to mechanical effects on cement in oil and gas industries, well movement is one of the most important factors that is affecting to cement integrity because of direct contact with wells. McCabe (1989) introduced a few types of vertical well movement as follow.

- Well Compression
- Thermal movement
- Platform Settlement
- Long term well settlement effect
- Equipment Failure

Ideally, casing movement should be restricted by the presence of a cement sheath, however, in a real world, it might not be always the case. The complexity of downhole condition as well as various operational steps will most likely lead casings to be dynamic.

The above factors will result mechanical effects on casings that end up resulting extra stress between cement and casing and most of the time. This unexpected

situation could make the cement weaken and it would end up resulting wellbore failures.

Until now, measuring the trend of compressive strength change on cement has been the most widely conducted test when it comes to study cement mechanics. In many different fields, including oil and gas industry and geothermal energy industry, investigations on compressive strength of various cement samples with variables such as thermal changes, variation in added additives, and curing time have been main interests in observing their relationship with well integrity issues.

For bonding stress, Kosinowski and Teodoriu (2012) conducted an experiment to observe the visible cement failure exposed to cyclic loads as shown in Figure 6. According to their experiment, the first crack was occurred as a radial crack. When the load on the sample was increased, more cracks were developed. And these cracks were grown as perpendicular to the initial crack starting near the middle of the cement sheath. After certain point of increased load, no more cracks were created, and it implies that the bonding between the cementing and the pipe has been lost.

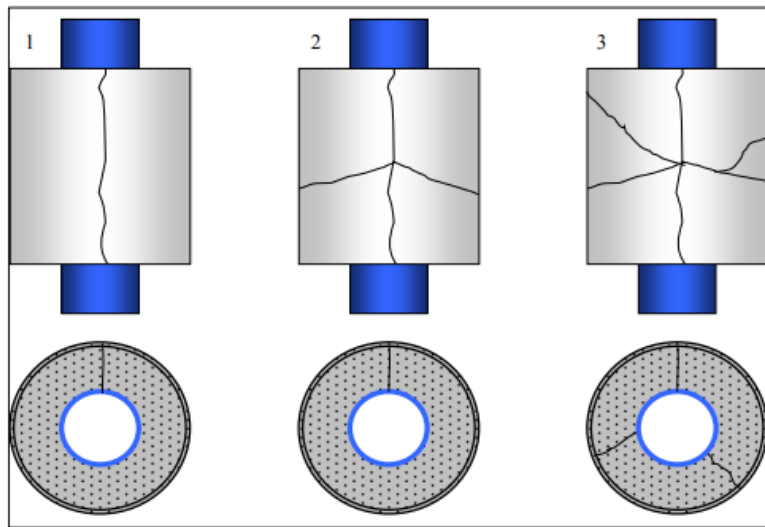


**Figure 5. Failure Sequence During Testing (Kosinowski et al, 2012)**

Wehling (2008) introduced the major mechanical issues affecting wellbore integrity related to the cementing are compressive, bonding, and shear failure as shown in Figure 6.

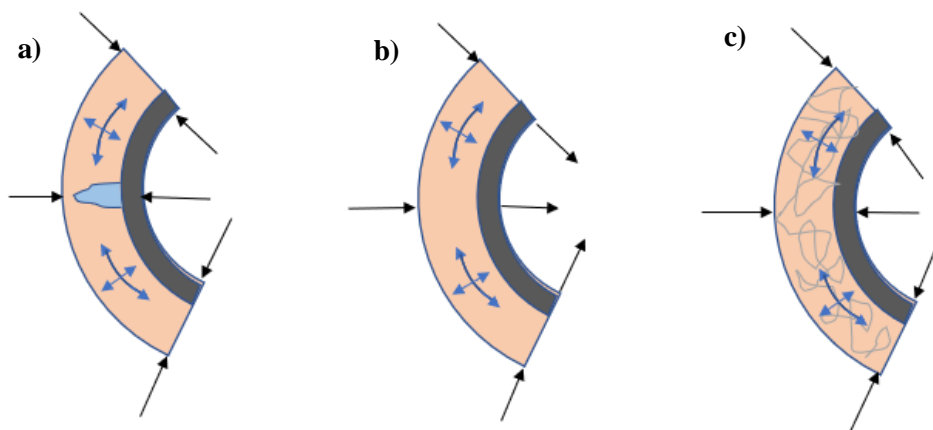


**Figure6. Types of Mechanical Cement Failure a) Radial Crack b) De-bonding c) Shear Failure (Wehling 2008)**

Thiercelin et al. (1997) and Philippacopoulos et al. (2001) mentioned that compressive strength might not be the main factor to be considered when we think of successful zonal isolation in oil, gas, or geothermal wells. These studies suggested that other mechanical properties of the cement, such as shear stress, bonding stress could also be important factors to consider when evaluating causes of well integrity issues.

For a better understanding, we must mention that the shear strength that is studied in this paper (cement pure shear strength) is a cement mechanical property similar to the unconfined compressive strength and the tensile strength. The bonding strength (also known as interface bonding strength) is an interfacial property that depends on cement and the other material that comes in contact with it (i.e. between casing and cement).

Because of the importance to understand shear and bonding strength in construction industries, concrete shear bonding strength has been studied in a various way. An example is shown in Figure7 that is a “Redrawn double shear push bond test”.(Haddad et al, 2013) However, a common setup for simulating shear stress in civil engineering is usually a beam shaped structure, that is different from the annular shaped cement placed in an oil and gas well. The results of such measurements are poorly related to the oil and gas cementing behavior as not be able to simulate cement-pipe interaction.

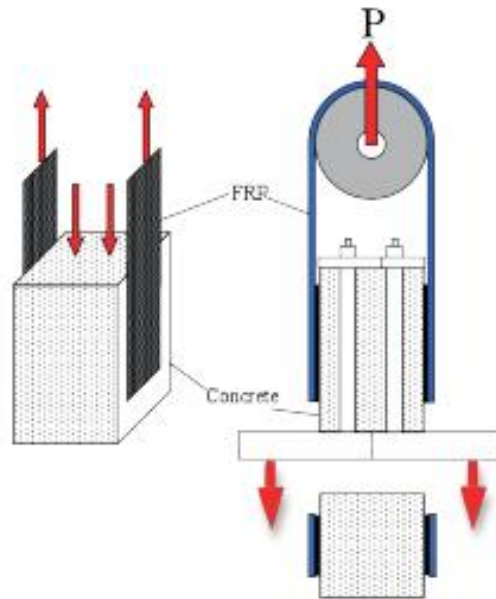


**Figure 7. Redrawn Double Shear Push Bond Test Setup (Haddad et al, 2013)**

Evans and Carter (1962) conducted bonding studies of cement to pipe, introducing the variables for different tests to obtain shear bonding strength and hydraulic bonding strength between casing and cement. They distinguished experiments between shear bonding and hydraulic bonding (which is not affected by shear stress). The shear bonding test is performed by measuring the force required to push a cylinder that was previously cemented inside of a cylindrical shape container. The hydraulic shear bond is measured by pumping water in the middle of two concentric cylinders that were cemented in place. Figure8 shows both experimental setups used by Evans and Carter (1962).

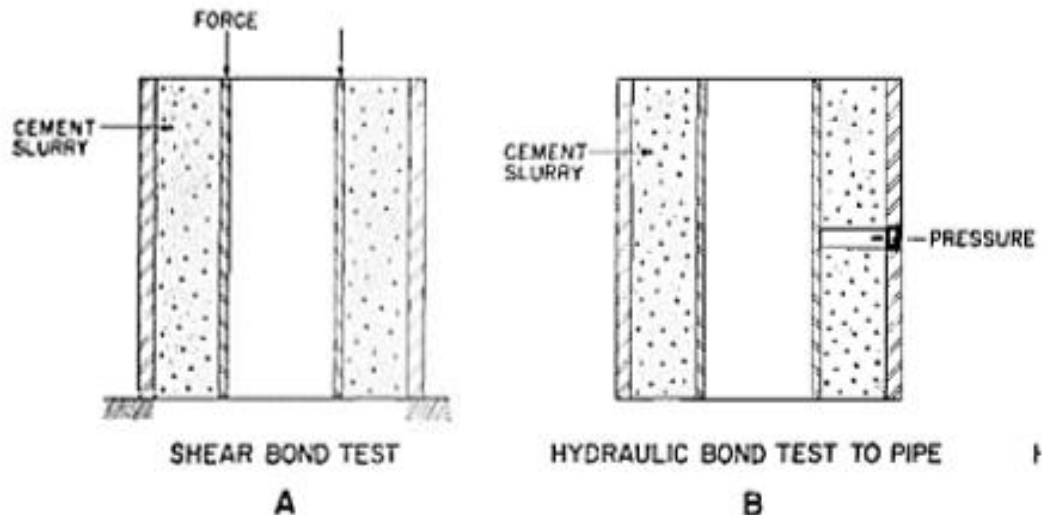


**Figure 8. Shear Bonding Test and Hydraulic Test Between Pipe and Cement setup (Evans and Carter, 1962)**

According to Nygaard (2014), lower bonding strength will lead to debonding at interface of casing-cement-formation as more dynamic loads are employed to the well.

Salehi et al (2016), stated that higher bond strength is desirable to prevent leakage paths at casing-cement-formation boundaries. In this paper, the authors defined bonding strength as a shearing force between the boundaries. The paper stressed that bond between cement and casing is a crucial factor for mechanical and chemical integrity of the wells.

It is also important to understand changing in cement chemical process when it come to cement bonding. According to Saleh (2018), the chemical process is more complicated and occurs shortly after cement powder exposed to water. The author

says that once cement is exposed to water, hydrates from and the hydration component of silicate phases is calcium hydrosilicate (CSH).

According to (Aïtcin and Flatt 2016), the composition of cement can be divided into four mineral components as follow:

- Tricalcium silicate:  $\text{SiO}_2 \cdot 3\text{CaO}$ , simplified C3S
- Dicalcium silicate:  $\text{SiO}_2 \cdot 2\text{CaO}$ , simplified C2S
- Tricalcium aluminate:  $\text{Al}_2\text{O}_3 \cdot 3\text{CaO}$ , simplified C3A
- Tetracalcium ferroaluminate:  $4\text{CaO} \cdot \text{Al}_2\text{O}_3 \cdot \text{Fe}_2\text{O}_3$ , simplified C4AF,

The authors stated that the hydration of cement result in mechanical bonding, heat liberation, and change of the cement paste volume, depending on the curing conditions. (Aïtcin and Flatt 2016)

Hydration of C3A is faster than C3S and this fast reaction dissipates hydroaluminum precipitates ( $\text{C}_3\text{AH}_6$ ). (Saleh, 2018) This calcium hydroaluminate result in premature stiffening of slurry. ((Gauffinet-Garrault, 2012) Shortly, tricalcium silicates come into contact and connected structure. (Saleh 2018)

Due to awareness of importance in securing a good bonding between casing and cementing, multiple researches have been conducted as substituting conventional oilfield cement to others. The Figure9 show the experimental results of using slag as a material. This study by Silva et al, (1997) states that the promising results were

found in the laboratory test and this slag-mix recipe can be used as an alternative to conventional Portland cement especially in conditions of moderate and high temperatures.

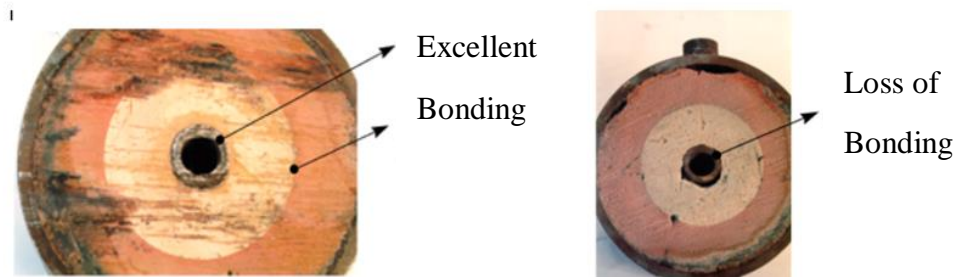


**Figure 9. Bonding difference using Slag Cement and Conventional Cement (Silva et al, 1997)**

Salehi et al, (2017) investigated shear bond strength of different slurry types from a lab scale experiment. In the experiment, Class H and Fly Ash Geopolymer slurries were compared. The result represented that shrinkage at Class H cement samples was visually detected after 12 hours of curing whereas Fly Ash Geopolymer sample showed little shrinkage as shown in Figure10.



**Figure 10. API Class H Portland Cement Sample (right) and fly ash geopolymer sample (left) prepare for shear bond testing. (Salehi et al, 2017)**

Any mechanical effect to the wellbore system is expected to spread out through the entire well casings, affecting to whole cementing system. All the above presented experiments refer to interfacial shear bond only. But since all casing strings rely on couplings to connect each joint, the cement-casing interaction in the coupling vicinity is different. We will need to discuss in this case about the pure cement shear stresses which are spotted near these couplings. The pure cement shear stresses occur because of the difference outer diameters of casings and couplings, see Figure 11.

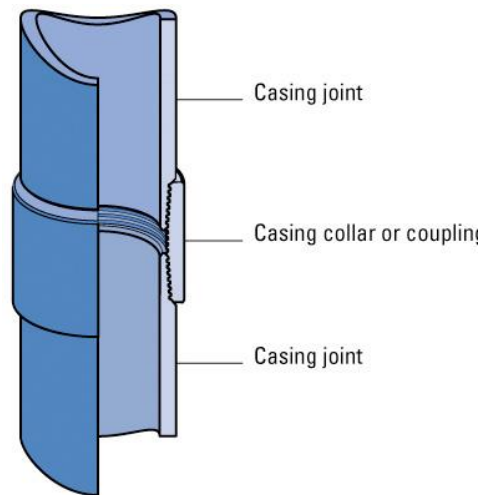


**Figure 11. Casing Schematics (Rigzone)**

In addition to casing vertical movement due to various reasons as we discussed, Teodoriu et al (2015), investigated cement failures related to casing fatigue in geothermal well. In this paper, he stated that, over the operational life of a well, the casing string is subject to external loads that can be considered static or quasi-static. However, unlike current industry design standards, it can be subjected to variable loads because of temperature change or internal pressure. According to Teodoriu(2015), the below casing fatigues can cause casing failures.

- Fatigue induced while running the casing
- Drilling induced fatigue
- Casing drilling
- Internal pressure induced fatigue
- Temperature variation induced fatigue

Analyzing casing fatigues relating to the cementing integrity is valuable because mechanical effects caused by casing fatigues would directly affect to the cement around casings. The theory of interaction between casing and cement can be described as this. The wellbore loads will induce movement or expansion to the casing at a displacement level higher than the cement, resulting into a relative movement casing cement. This relative movement induces initially stresses at the casing cement interface until these stresses will exceed the interfacial bonding stress.

This extra stress would result because of some special loads at the area where the geometry of the casings is changed. The main changes in geometry in one cementing system would be the location where cement is sheared rather than debonded. These abnormal loads will directly affect to cement near the area and will cause mechanical issues on cement. One of important special loads that occurs at the coupling cement contact would be pure cement shear stress.

### 1.3 Objectives

First, this thesis research simulated the special loads that are likely to be found at the area where the geometry of casing-cement is changed. More specifically, this study focuses on a spot where a coupling connects two joints of casings. Lab sized experiments using Portland Class H cement were performed in order to observe special forces near the coupling area, and to acquire a better idea of cement

mechanical behavior near the coupling area. Also bonding stresses between casing and cement were observed in order to link to the cement pure shear stress at coupling area. UCS test was also conducted as a purpose of comparisons to both shear and bonding stresses.

In short, bonding, shear and unconfined compressive strength of Class H cement will be compared.

The curing time was selected as 1day, 3days, 7days, 14days, and 147days (long term behavior) to see the changed of cement mechanical testing results. Lastly, elevated temperature ( $65\pm 3$  °C) was applied as a curing environment (no pressure change) to compare to ones that were cured at the room temperature.

The main objectives of this work are:

- Evaluating pure cement shear stress near coupling installed area and its trend as time changes
- Evaluating bonding stress between casing (near coupling) and cement and its trend as time changes
- Evaluating cement UCS with time change manner
- Analyzing the obtained shear, bonding, and UCS values and compare their changing trend as a time change manner.

## **2. Wellbore integrity and Wellbore cement**

This section introduces the well integrity, the basic operational process of wellbore cementing, importance of cementing in terms of wellbore integrity, oilfield cement classification, and casing/coupling mechanics

### **2.1 Life of well, Cement, and Wellbore Integrity**

Throughout the entire well life, wellbore integrity is probably the most important thing to be paid attention since it directly relates to human, environmental, and cost related issues. The well life starts from a well construction phase and end at a stage of abandonment. The main goal of well construction is to reach the target depth the most safely and cost-effective way and to result the most efficient output throughout the well lifetime. It usually includes drilling and a part of completion prior to a stage when the production casings are installed. After a well construction phase is completed, hydrocarbons are extracted during a phase of production. This phase would go through dynamic changes in mechanical, chemical or even geological variations that would affect to casing behaviors. When a well is abandoned, the importance of well integrity still need to be secured due to government regulations of environmental, health, and humanitarian concerns.

Well integrity is defined as the application of technical, operational and organizational solution to reduce the risk of uncontrolled release of formation fluids throughout the life cycle of a well (NORSOK, 2004).

API states that casing must be able to withstand the various compressive, tensional, and bending forces that are exerted as well as the collapse and burst pressure that might be subjected to during different phase of the well's life. (API, 2009) Wellbore cement is placed between casings and formations and it is shown in Figure12. (Drilling Course,2015)

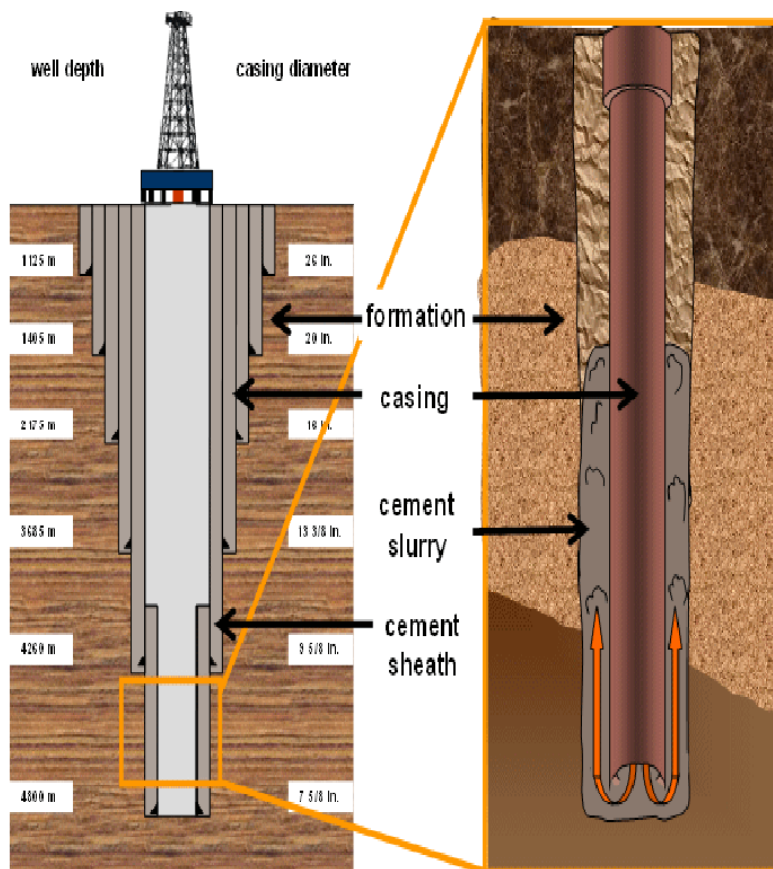


**Figure 12. Wellbore and Cement (Drilling Course, 2015)**

Likewise, if we understand the close relationship between wellbore integrity and casing behavior, it is easy to expect that wellbore cement is directly affected by

casing behavior due to their direct physical contacts. However, as mentioned above, the casing behaviors are caused due to unpredictable downhole conditions (pressure, temperature), chemical reaction, corrosion and production scenarios that are dynamic. Therefore, it is hard to expect a perfect well with zero wellbore integrity issues.

According to Davies et al. (2014), up to 75% of the well encounter well integrity issues or barriers depending on the area and the number of wells studied. Likewise, wellbore integrity issues cannot be ignored in the industry.

There have been a few major incidents related to wellbore integrity issues in oil and gas industry. One of the most memorable events of wellbore integrity related incident would probably a Macondo happened in 2010 in Gulf of Mexico. This tragedy happened when a well control even brought hydrocarbon fluids into the Macondo well and then onto the Deepwater Horizon semisubmersible. (Santos et al, 2017)

According to BP's report (2010), Failing to stop the flow and the rig exploding lead 11 people to die, 17 people to get injured, and caused a serious oil spill. After 36 hours of explosion, the semisubmersible sank and the well continued to flow for 87 days. The investigation says that the accident involved various reasons from human factors to technical factors that caused loss of well integrity. Moreover, lots of oil field specialists and researchers have figured out that inappropriate cement job was

one of most crucial failure factors caused loss of wellbore integrity. The below show the possible cementing failures contributed to Macondo incident. (Benge 2013)

- Heavy dry cement for its geology could have fractured rock formation
- Less stabilizers were used than recommended number (Improperly placed cement)
- Inadequate cementing design
- Pouring cement in a hurry before giving a time to return to the normal temperature
- Less amount of cement used

According to Benge (2010), cementing wells is a complex endeavor and industry experts inform us that cementing failures are not uncommon even in the best of circumstance.

## 2.2 Wellbore Cementing Fundamentals

From raw cement on the surface (oilfield) to cementing slurry that is placed in a well, the brief process is shown at the diagram in Figure 13. Depending on cement design, a specific base cement is selected along with various dry additives. The dry materials go to a bulk blender and the water is also added. In order to produce wet cement (slurry), they are mixed by various kind of mixers. Usually Portland cement is used in oil fields that is one of API classes cement. Various additives can be

added according to various situation. The details of additives will be introduced in the next chapter. After casing construction has been done, the mixed slurry is pumped into the well.

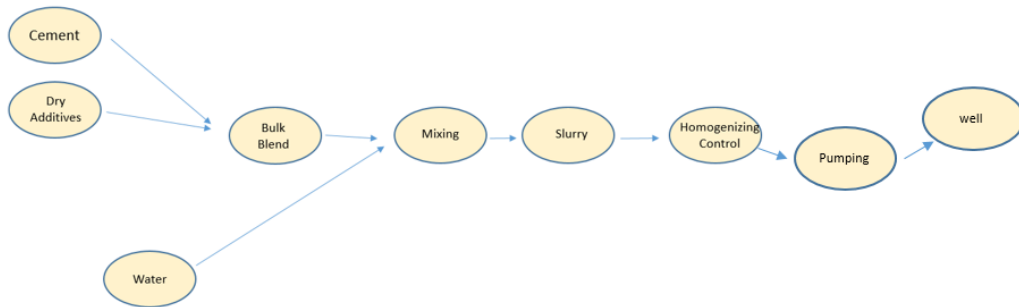


**Figure 13. Oilwell Cement from Surface to Wellbore**

Wellbore cementing mainly consist of two stages, primary cementing and secondary cementing. Primary cementing is performed immediately after the casing is run in the hole to obtain an effective zonal isolation and to help protect the pipe.

According to Smith (1974), cementing also helps in:

- Bonding the pipe to the formation
- Protecting production strata
- Minimizing the danger of blowouts from high pressure zones
- Sealing off “lost-circulation zones” or other troublesome formations as a prelude to deeper drilling

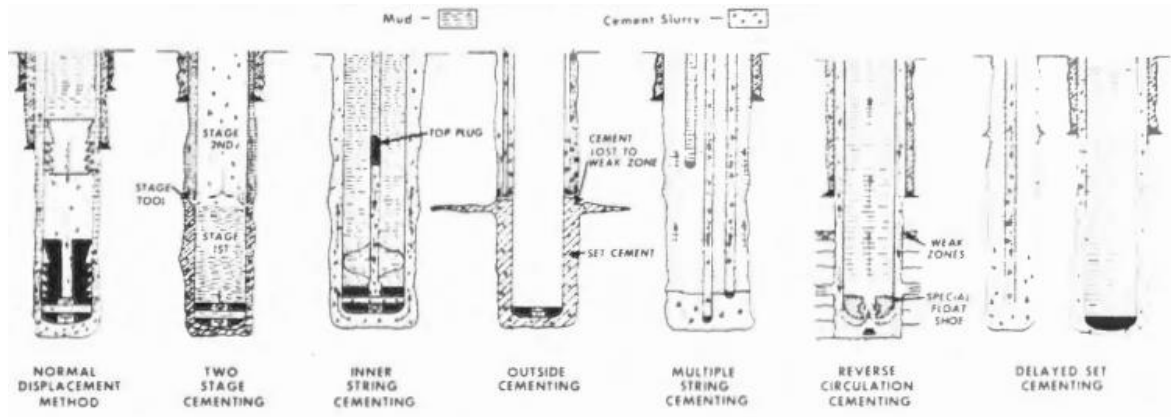


**Figure 14. Placement Techniques for Primary Cement (Smith 1974)**

Figure 14 shows various types of primary cement operational methods.

According to Hole (2008), inner string casing, and reverse circulation casing are main ones among various techniques of primary cement methods, through the casing.

Secondary cementing, which is also called squeezing cementing is required to maintain well operability. (Ichim 2017) Secondary cementing can repair a faulty primary cementing, stop drilling fluid losses, seal abandoned or depleted formation, and repair casing leaks. (Fink 2015)

### 2.3 Wellbore Cement classification

Oilfield cements are manufactured to comply with API Spec 10A (Specification for Cements and Materials for Well Cementing) and tested according to API RP 10B-2 – Recommended Practice for Testing Well Cements. The Portland cement is classified as below according to the API.

**Table 1. Portland Cement Class (Nelson and Gulliot 2006)**

Class	Depth (ft)	Temperature F	Purpose
A	0-6000	80-170	Used when no special needs are required
B	0-6000	80-170	Used for conditions requiring moderate to high sulfate resistance
C	0-6000	80-170	Used for conditions requiring high early strength
D	6000-10,000	170-290	Used where high temperatures and pressure are found
G	0-8000	-	Used with accelerators and retarders to cover all range of well depth and temperatures
H	0-8000	-	Used with accelerators and retarders to cover all range of well depth and temperatures

Portland cement is used for oilfield cementing due to the cost effectiveness and easy obtaining. As shown in Figure 15, the basic materials of the Portland cement are argillaceous and calcareous rocks. (Ichim 2015) In order to create the Portland cement, the base rock is heated in a high temperature that is range of (2600 F-2800 F), and the materials get to form a clinker. Then the clinker is mixed with other products such as gypsum. (Nelson 1990) This is called Portland cement. The composition of the raw materials, length of exposure to heat, maximum kiln temperature, and rate of cooling all affect the phases present in the clinker.

(Polkowski 1987) By adding water into the Portland cement, the basic cement slurry is formed.

The amount of water that is added to the cement varied with the size of particles, and it is very important to consider the amount of the water to add to the cement because excessive water can the cement slurry oversaturated and the water will be remaining on the top of the cement slurry not mixed with cement completely. (Saleh 2018)

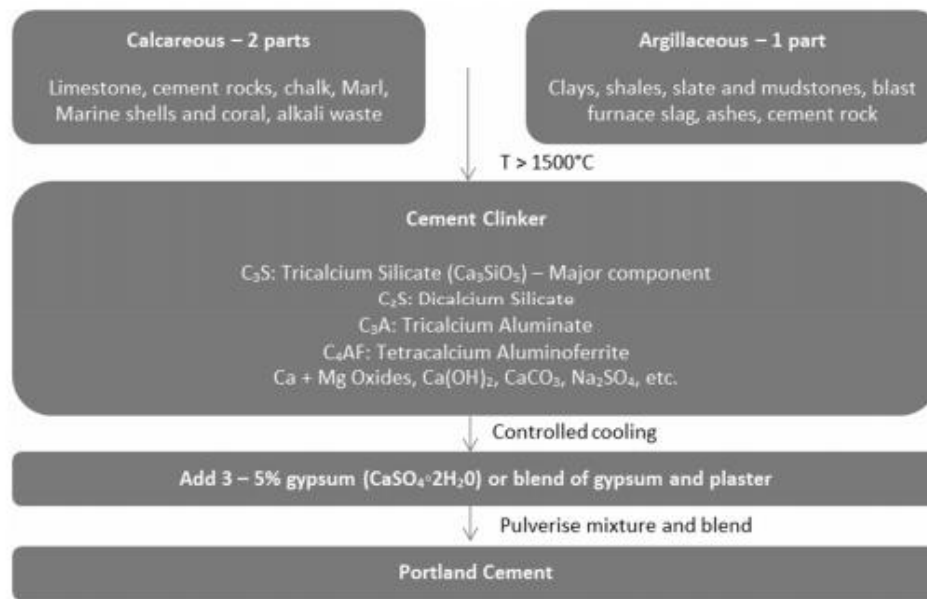


**Figure 15. Portland Cement Production Workflow (Ichim 2015)**

Each of categorized cement contains different portions of elements of various oxides, silica, and alumina. Polkowski investigated the details of element

compositions in each class of Portland cement as shown in Figure16. (Polkowski 1987)

Elemental Composition by EDS

Element	Weight Percent					
	Cement A	Cement B	Cement C	Cement D	Cement E	Cement F
Na <sub>2</sub> O	0.50	0.22	0.10	0.00	0.14	0.14
MgO	0.78	1.45	0.90	1.27	0.96	0.89
Al <sub>2</sub> O <sub>3</sub>	4.11	4.01	3.68	3.43	4.42	3.77
SiO <sub>2</sub>	19.61	20.74	19.42	20.52	19.37	21.08
SO <sub>3</sub>	6.20	3.73	4.15	5.01	4.34	5.04
K <sub>2</sub> O	0.97	0.64	0.21	0.38	0.53	0.41
CaO	64.87	64.22	67.21	64.46	64.12	64.15
SiO <sub>2</sub>	0.13	0.14	0.12	0.19	0.23	0.11
Fe <sub>2</sub> O <sub>3</sub>	2.82	4.85	4.20	4.74	5.99	4.41
TOTAL	99.99	100.00	100.01	100.02	100.00	100.00

**Figure 16. Element Composition in Various Portland Cement Class (Polkowski, 1987)**

The composition studied by Polkowski is also supported by a study of Fink.(2015) He summarized a general composition range of the Portland Cement and the result is matching with the study conducted by Polkowski.

- CaO (Calcium Oxide): 60-69%
- SiO<sub>2</sub> (Silicon Dioxide/ Silica): 18-24%
- Al<sub>2</sub>O<sub>3</sub>(Aluminum): 4-8%
- Fe<sub>2</sub>O<sub>3</sub> (Iron Oxide) : 1-8%

- MgO (Magnesium Oxide): <5 %
- K<sub>2</sub>O, Na<sub>2</sub>O (Potassium and Natrium Oxide): <2%
- SO<sub>3</sub>(Sulfur Trioxide/Sulfite): <3%

Solid form of cement may include various additives such as dispersants, polymers, fluid loss, weight agent and special additives to obtain optimal cement design for various situations. Cement additives can be categorized as shown in Table 2. (Nelson 1990)

**Table 2. Various Additives, Purpose of Use, and Main Functions (Nelson 1990)**

Purpose of Use	Main Function	Additive
Density Reduction	Reduce Cement density Prevent formation fractures	Bentonite, Clay minerals
Weight materials	Increase slurry's density	Barite, Hematite, Sand
Viscosifier	Reduce viscosity of slurry Prevent fracturing while cement being pumped	Sodium Chloride, Calcium lignosulfonate
Filtration control	Prevent leakage	Caustic Soda, Calcium hydroxide
Accelerators and	Reduce settling time	Calcium chloride, Sodium chloride, Potassium chloride
Retarders	Increase settling time	Calcium lignosulfonate Cellulose.

## 2.4 Cement Shear Bonding Strength Mechanism

Bonding between cement and casing is a crucial factor for oil well integrity.

Bonding of cement and steel can be described as adhesion because the material surfaces are contacting and stick together. In this chapter, various adhesion mechanisms will be introduced.

### 2.4.1 Intermolecular Bonding

Intermolecular bonding which is known as van der Waals forces is caused from molecular contact between two materials and the surface forces. (Bwala 2015) states that the adhesive must make intimate, molecular contact with the substrate surface for forces to develop. "Wetting" is a term of maintaining continuous contact between an adhesive and an adherent. According to Bwala (2015), permanent adhesion results from molecular attraction forces after contact between adhesive and adherent through wetting.

### 2.4.2 Chemical Bonding

Chemical bonding of adhesion includes ionic, hydrogen bond or covalent formed at an interface.

### 2.4.3. Mechanical Bonding

Surface pores generated by the roughness that are occupied by adhesive materials allow surfaces to attach together. Adhesion occurs when adhesive fills on surface

voids. As adhesive gets harden, it holds the substrates together. This is a mechanical bonding theory. Surface roughness is crucial factor to affect to adhesion due to the change of contact area between adhesives and the adherent depending on surface roughness.

### 2.5 Thesis Idea

Wellbore cement mechanics play an important role when it comes to wellbore integrity. As the diagram in Figure 17 shows, cement mechanical damage causing a loss of well integrity appears after cement settles and becomes solid.

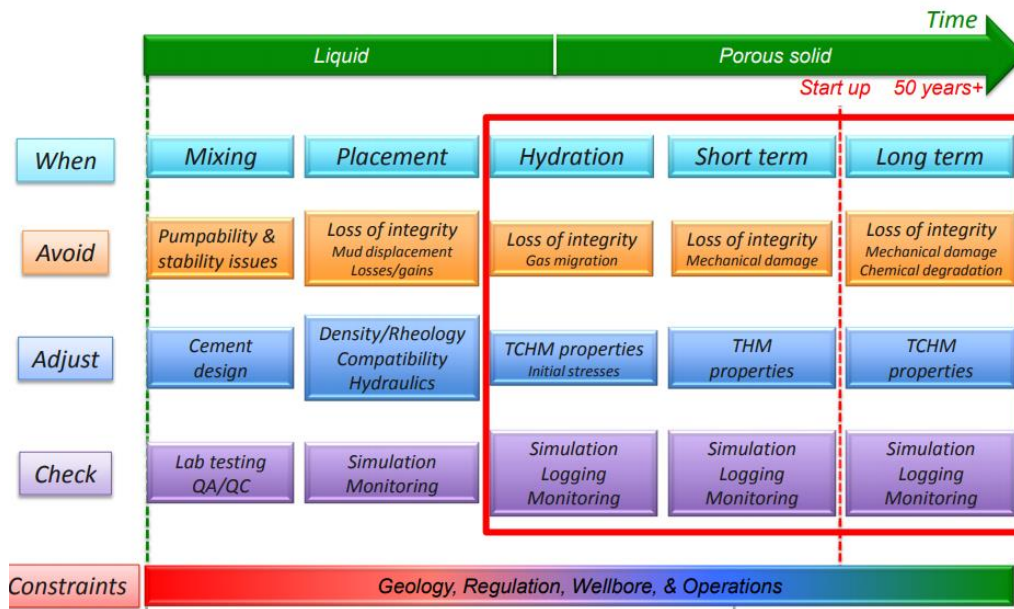


**Figure 17. Change of Wellbore Cementing Phase (Drilling Info, 2015)**

Cement slurry is injected into wellbore as liquid (slurry). When injected slurry gets dehydrated, the liquid form is changed to solid as it gets settled between well

casings and formations. Mechanical issues on cement get started from this phase and the wellbore integrity issues related to cementation start to appear. Not only for a short term, it is considered as a long-term issue.

In terms of cement mechanical issues in wellbore environment, de-bonding between cement and casings have been considered as a main problem. However, there might be additional special stress near couplings are installed due to difference in geometry of casing and coupling. In Figure 18, B represents the bonding stress between casing and cement. However, the area that is indicated by A should have additional stress as casing moves up caused by axial load from casing. We call this special stress as “Pure cement shear stress”. This thesis idea is summarized as the Figure18 and we will investigate each of pure cement shear stress and (shear) bonding stress between casings and cement and their possible relationship in the next chapters.

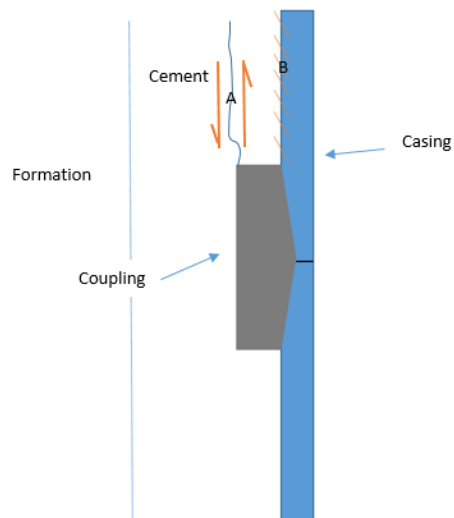


**Figure 18. Cement Shear (A) and Bonding Stress (B) near Coupling**

### 2.5.1 Shear Fail mechanisms

In a subsurface environment, shear failure mechanism is complicated due to heterogeneous formations. Maurer (1965) investigated the correlations between shear stress and normal stress. He obtained the result as the shear strength increases as the normal stress increases representing a shape of typical Mohr's diagram from compression tests.

According to Nygard (2007), shear failure doesn't always result fracturing for rock. Not only affected by shear failure criterion, shear fracturing is also affected by ductility or brittleness. A type of deformation depends on the properties of material and the effective stress level. Ductile behavior starts as contractive respond and it becomes to failure when stress reaches to the failure point. Similarly, Maurer (

1965) concluded that the transition from brittle to ductile failure occurs when the friction along the fracture surfaces exceeds the shear strength of the rock. Figure 19 shows a graph of the transition from brittle to ductile. The same theory can be applied to cements, thus the shear strength of the cement must be first measured and documented. This thesis will focus on measurement of cement shear strength,

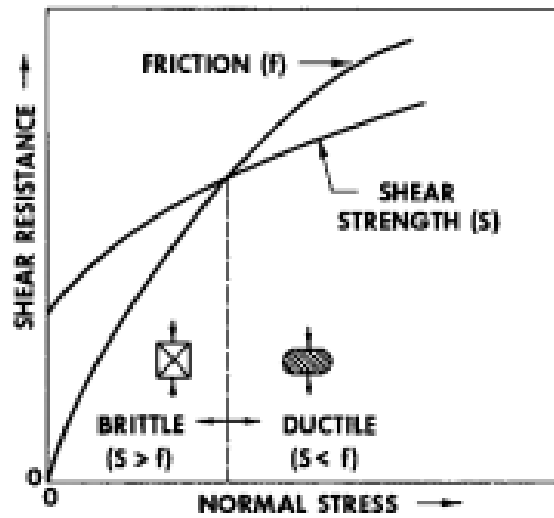


Figure 19. Transition from Brittle to Ductile. (Maurer 1965)

### 3. Experiment

Portland Class H cement was used for this study without any additives included. Class H was used as it is the most common cement used in GOM (Gulf of Mexico) recipes.

The amount of water used to make the cement mixture (or slurry) was 38% by weight of well cement (Class H, according to API Spec 10A). Since there are no API standardized test setups for obtaining cement pure shear stress or bonding stress between casing and cement, proper cells were customized. Samples were cured for a day, 3 days, 7days, 14days and 14 days before pure cement shear, bonding, and UCS tests. In addition, the same samples for 3 days testing were prepared for high thermal effect comparison. The same cement has been used for the high temperature shear and bonding samples but only difference was the curing temperature of  $65C \pm 2 \text{ } ^\circ\text{C}$ .

Each batch has 2 samples of shear and bonding specimen. In order to secure large population of specimen, 3 trials of the same curing day test were done for 1 day, 3 days, 7days sample. For 14days and 147 days, one trial was conducted due to limited time. For UCS test, each batch has 3 samples, and the trial number was applied the same as shear and bonding test. For 3 days high temperature test, 2 trials were conducted for shear and bonding test.

### 3.1 Cement Mixing

A method of mixing cement has been recommended by American Petroleum Institute (API). We used the OFITE automate cement mixing unit and a bladed blender.

600 ml of cement slurry was prepared. 860.26 g of Portland Class H cement and 326.90 g of deionized water is mixed in the one-quarter cup. According to Saleh et al(2017), mixing energy variation affect to cement mechanical properties. Therefore, it is important to follow the recommended mixing energy values of 5.9KJ/Kg. (Ichim,2018) The mixing temperature is a room temperature of  $22C\pm 1^{\circ}C$ . The water and cement weight were measured separately before they are mixed. API suggest mixing schedule to be 4,000RPM $\pm$ 250RPM for 15 second and increase the RPM to 12,000RPM $\pm$ 250 RPM for 35 second. The time for mixing makes 50 second. The maximum deviation that electronic control unit ensures is  $\pm 50$  RPM. (API, 2013)

To calculate mass of cements and water for specific volume, the below equation is used.

$$\rho \text{ slurry} = \frac{M \text{ total}}{V \text{ total}} = \frac{M \text{ Cement} + M \text{ Water}}{V \text{ Cement} + V \text{ Water}} \quad (1)$$

In order to prepare 600 ml Class H cement slurry with a slurry density of 1.98 kg/L (no additives), the required water and cement mass were 860.26g and 326.90g each.

For all experiments in this thesis, only one kind of cement slurry was mixed by API mixing unit recommendation, API 10D.

1. Measured mass of deionized water (326.90g) and Portland class H cement (860.26g).
2. Pour measured deionized water to a mixing cup.
3. Start the mixer that contains deionized water. The mixer is set with a rotational speed of 4,000RPM for 15 second and 20,000RPM for 35 second. For the first 15 second phase, the measured cement should be added.
4. The lid should be placed within the 15 second phase to ban the mixing slurry splashing. The mixing speed of the mixer will increase to 20,000RPM for 35 second.
5. After the mixer stops, remove the lid and pour the cement slurry into the molds.

### 3.2. Cement Curing

The density of the mixed cement slurry is measured before it is poured to the molds.

In this process, the cement slurry is well mixed following the API requirement. If the density varies too much, the outcome from mechanical testing would not be

correct. Typically,  $\pm 0.1$  SG would be accepted as an error that could be caused by various reasons such as air bubble trapped inside the cement slurry, variation in chemical densities in cement, and varying water density. (Ichim,2018)

The cement slurry is poured into each of the two customized molds for shear and bond test as well as standard 2in X 2in cement cube molds, see Figure 20.

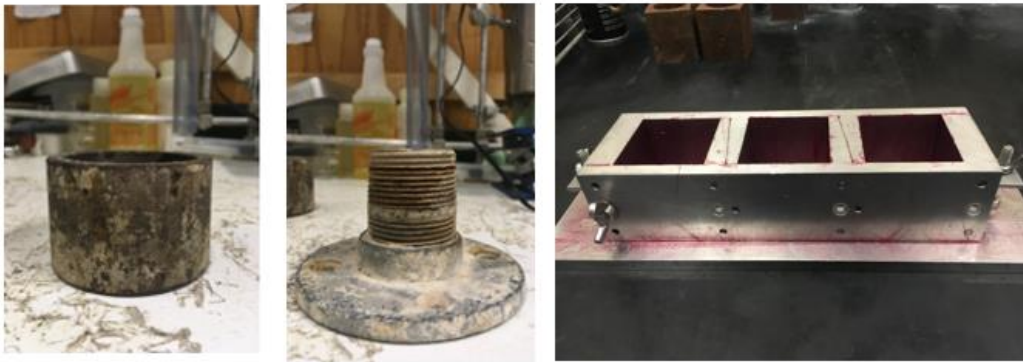


**Figure 20. Shear (Left), Bonding (Center), UCS Cubes (Right) Molds**

The pure shear mold and cube mold are coated with a watertight release agent (grease) for different reasons. For shear mold, the aim of this test is to see only shear strength that should not take in account the material surface, therefore the grease was applied. For the cube mold, the grease is simply because of an easy removal and preventing slurry loss.

The slurry is poured into the prepared molds carefully. To minimize trapped air bubble in the cement, the cement is poured up to half of each molds, then with using

a spatula, the half way filled cement is stirred. After this step, the remaining cement is poured to the top of each mold.

The molds filled with cement slurry are placed in deionized water bath. In this particular experiment, the water temperature was set to be room temperature range of 20-22°C and atmospheric pressure. For a comparison purpose, using the thermal effect water bath, 3 days curing samples were placed in the special thermal bath set to maintain the water temperature of  $65\text{C}\pm 3^\circ\text{C}$ .

The cement cube samples cured in API standardized molds were removed from the molds after a day and were kept in the same water until the designed schedule testing day. The cement in the shear and bonding molds are stayed as they are cured until the test because both properties are dependent of either mold design or mold material as shown in Figure 21.



**Figure 21. Experimental Samples Curing in Room Temperature Water**

In order to investigate cement behaving in high temperature environment, the curing bath shown in Figure 22 is used. We prepared shear and bonding samples of 3 days curing at  $65\text{C}\pm 3^{\circ}\text{C}$  for a purpose of comparison to the 3 days curing samples at room temperature ( $22\text{C}\pm 2^{\circ}\text{C}$ ).



**Figure 22. Hot Tub (Left) for High Temperature Curing and Samples (Right)**

### 3.3 Cement Sample Geometry

Since there is no API standard geometry for shear and bonding test, the moldings were customized to make it simpler to test out in a laboratory sized experiment. Even though various researches attempted to measure pure cement shear stress and bonding stress (interface shear stress) with various setups, this experimental setup that is introduced in this paper can be stated as the simplest yet effective.

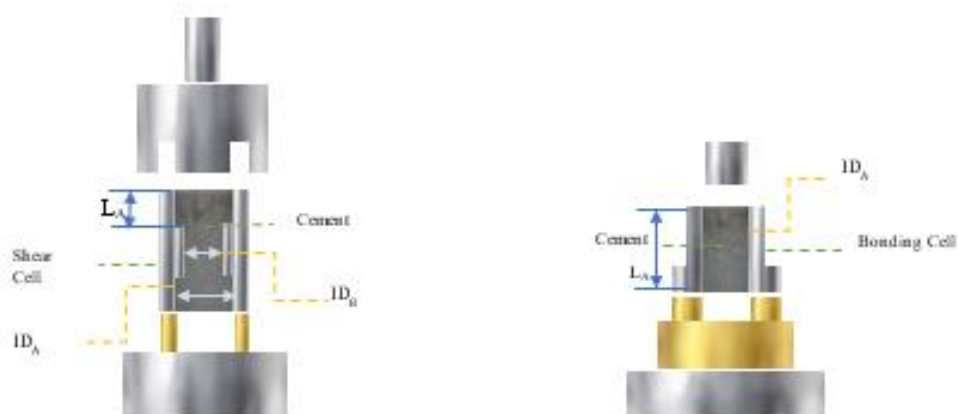
The outer diameter of casing simulating part and coupling simulating part were not scaled as size ration of industry uses. However, we believed that this simplified simulation would explain the behavior of cement and the area where the coupling is installed on the joint of two casings.

Figure 23 shows bonding, shear and UCS sampled after each testing has been done.

Figure 24 shows cut off schematics of shear and bonding cells.



**Figure 23. Bonding (Left), Shear(Center), UCS cubes(Right)Samples after Testing**

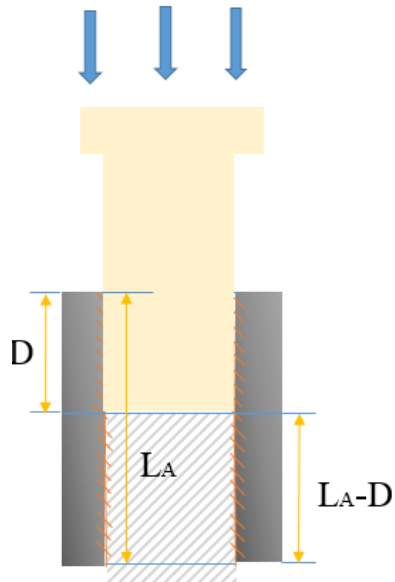


**Figure 24. Shear (Left) Cell Cut-Off Diagram, Bonding (Right) Cell Cut-Off Diagram**

**Table 3. Geometry of Shear and Bonding Cells**

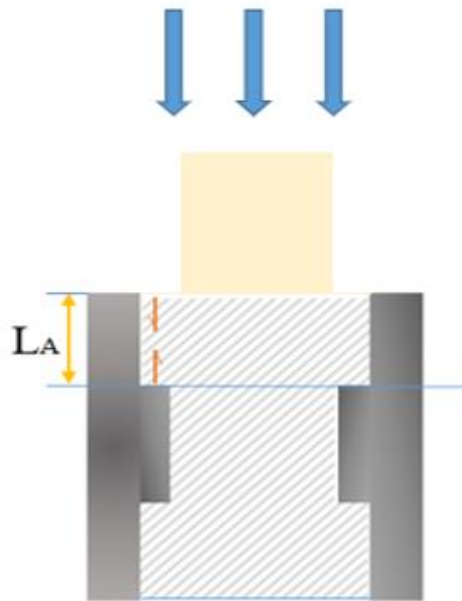
	Affected Length (L <sub>A</sub> ) (mm)	Outer Diameter (mm)	Inner Diameter (IDA) (mm)	Inner Diameter (IDB) (mm)
Shear Cell	16.1	75.6	61	54
Bonding Cell	50- D	40	35.1	-

Table 3 shows geometry of shear and bonding cells that were used for the entire experiment. “D” is measured displacement which varies as the hydraulic pressure is applied and the cement inside of the bonding mold is displaced. Since bonding strength is closely related to the surface area of the inside of the bonding mold, where cement is contacted, the affected area is calculated account to the displacement changes. The below diagram explains about more details of displacement concept in bonding mold. As shown in Figure 25, the bonding stress will be observed where the mold and cement has contact area. Therefore, for bonding stress calculation, the length to calculate the contact area will be the entire mold length where displacement shows zero subtract to the displacement value.



**Figure 25. Bonding Stress Diagram Showing Displacement and Length**

Shear test has different principles to bonding test. In a geometry point of view, shear stress is nothing to do with the contact area between cement and shear mold. Rather, the part that shear stress is occurring would be the interest point that determines value of length when it comes to the shear stress calculation.



**Figure 26. Shear Stress Diagram Showing Length**

According to API standard, the ideal size of cement cube for compressional strength testing would make 2 in x 2 in sharp. However, each cement cubes have slightly different shapes and sizes even though the size of even molds is uniformly designed and manufactured according to the API. The form deformation or size changes usually happens when molds are cured in the water curing bed. Water could be washed out a top part of cement slurry poured into molds. Therefore, the size of width and length of each cement specimen has been measured by using digital Vernier Caliper.

In order to obtain more accurate result, width and length have been divided into 3 and the final values that are used for the compressive test was an average value of each of 3 measurements, see Figure 27.

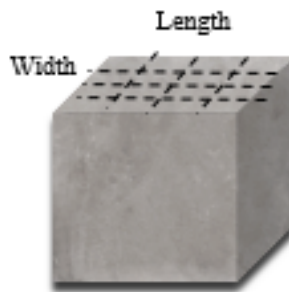


**Figure 27. UCS Cubes Length and Width**

### 3.4 Mechanical Strength Test

Both of pure cement shear and bonding strength were measured using a hydraulic press with a maximum capacity of 20tons, see Figure 28. This H-Frame Industrial Heavy Duty Floor Shop hydraulic press manufactured by Central Machinery is known as having 0.1% error of both load cell and the displacement cell. This error percentage are considered when we analyze the obtained data.



**Figure 28. Hydraulic Press (Central Machinery)**

For a result display purpose, a data acquisition software, DASyLab, was used as shown in Figure 29.

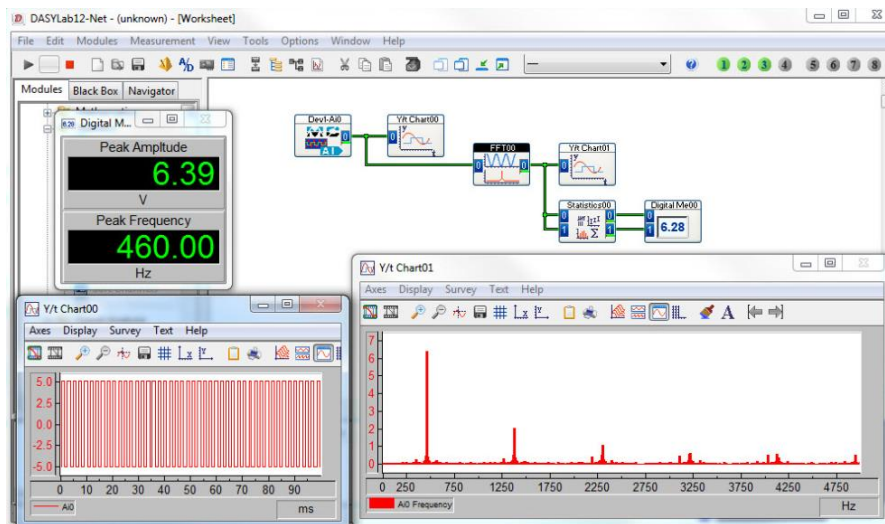


**Figure 29. DASyLab**

This software was calibrated to show the force gauge and displacement to be calculated to present shear and bonding force (MPa). A force gauge placed at the bottom measures the axial load applied on the samples, while the attached displacement sensor measures the cylinder displacement. Displayed force gauge on DASYLab was then calculated to real force using a calibrated gauge and a correlation was generated as a quadratic function with a variable of obtained force gauge. The force was calculated to stress using each cell's geometries. Cells to use to acquire shear and bonding stress were customized having their own adapter to apply force only on the cement. The calculation methods to obtain stresses and each geometry of cells will be covered in the subcategory in this chapter. In this experiment and analysis, unit was united as SI unit.

### 3.4.1 Pure Cement Shear stress



**Figure 30. Shear Stress Setup (Left), Shear Mold Front View (Center), Inside View (Right)**

The hydraulic press has been used to apply loads on the customized shear stress testing cells, see Figure 30. The values that we obtain from the shear setup are displacement and gauge force. The results are shown on a computer screen which the DASYLab has been installed. Then the gauge forces are plugged into the correlations to obtained force. This force is used to calculate stress using the mold geometry that was shown at the previous sub chapter.

$$\sigma = \frac{F}{A} \quad (2)$$

For the pure cement shear stress test, the interest area of the shear cell is not the entire length but the length from the top to the spot where the coupling shoulder starts (from the top). Also, because this test has nothing to do with the contact area between cement and the metal, the surface area where cement and casing contact stays the same when the cement shear stress is calculated.

The material of customized shear cell is stainless steel with low pipe roughness. Since shear stress has nothing to do with the cell material itself, and should avoid having bonding with cement, the inside of the cell that is a contact area with cement was greased.

### 3.4.2 Bonding stress



**Figure 31. Bonding Stress Setup (Left), Bonding Mold Front View (Center), Inside View (Right)**

To apply loads on the bonding cells, the same hydraulic press that is used as one for the shear test, see Figure31. However, the cells for bonding stress test have different geometry to those for shear stress test, see Figure24. This is because the principle behind the shear and bonding test is different. For bonding test, the manufactured material of casing matters to the cement-casing bonding stress. Therefore, no grease was applied on the surface area that is contact to cement. In this experiment, the bonding cell was made out of a zinc plated structural pipe to obtain a good bonding between the cell and cement.

Bonding stress calculation needs to consider the displacement of cement while hydraulic press is activated and applies forces towards cement. This is because the

bonding stress is directly affected by the surface material. Therefore, when cement inside of the bonding cell is removed and relocated, the length that is used to calculate the relationship between the metal material and cement should be changed.

The affected length in bonding stress calculation is going to be kept in change as displacement cell measures different values.

### 3.4.3 Unconfined Compressive Strength (UCS)

Unconfined compressive strength of the cement cube specimen has been measured by CM-2500 (Figure32) manufactured by Test Mark Industries.

This device applies uniaxial load to the object and measures the minimum necessary force to cause a plastic deformation of the object. The unconfined compressive strength machine has an accuracy of  $\pm 0.5\%$ , and it will take account when shear stress is calculated later on the next chapter. In this experiment, the object was cement cube specimen that was corresponding to the curing days of specimen for shear and bonding stress measurement.



**Figure 32. CM-2500 Compression Testing Machine (Romanowski et al, 2017)**

This test was conducted mainly to compare the trend of compressive strength according to the trend of shear and bonding stress. For compressive strength calculation, three width and length were measured to obtain the average value of width and length of cement cubes (Figure 27). Using the average length and width of each cement cubes, the surface area was calculated.

#### 4. Acquired Data and Analysis

##### 4.1 Correlations

The force gauge was calibrated against a certified force gauge. The force gauge used for this experiment showed a slight non-linear behavior for high end, and therefore the calibration was made using a second-degree polynomial correlation, as shown in Figure 33.

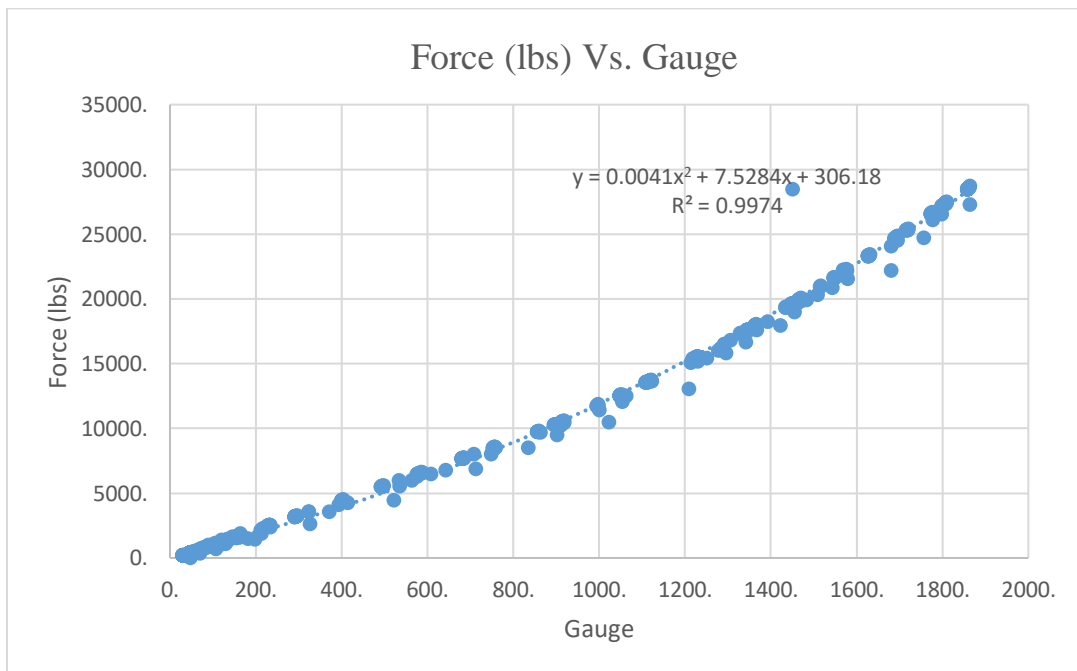


**Figure 33. Proposed Correlation of Force Vs. Gauge**

By using the proposed correlations,

$$y=0.0041x^2 + 7.5284x+306.18, R^2=0.9974 \quad (3)$$

shear and bonding forces were calculated throughout the experiment. The gauge values were plugged into the correlation and the result value were converted to force in the unit of pound force (lbf). Since we use SI unit for all calculations, pound force was converted to Newton (N).

#### 4.2 Calculation Method

By using the hydraulic press, axial force and displacement values were obtained. An example of the raw data is shown in Figure 34 for the 3days curing sample. The failure force is measured as the maximum indicated force on the graph, before abruptly drops (See the marked point in Figure 34). Likewise, every test was plotted in a same way, and the maximum force shown before abrupt drop was correlated to the where stress failure was detected.

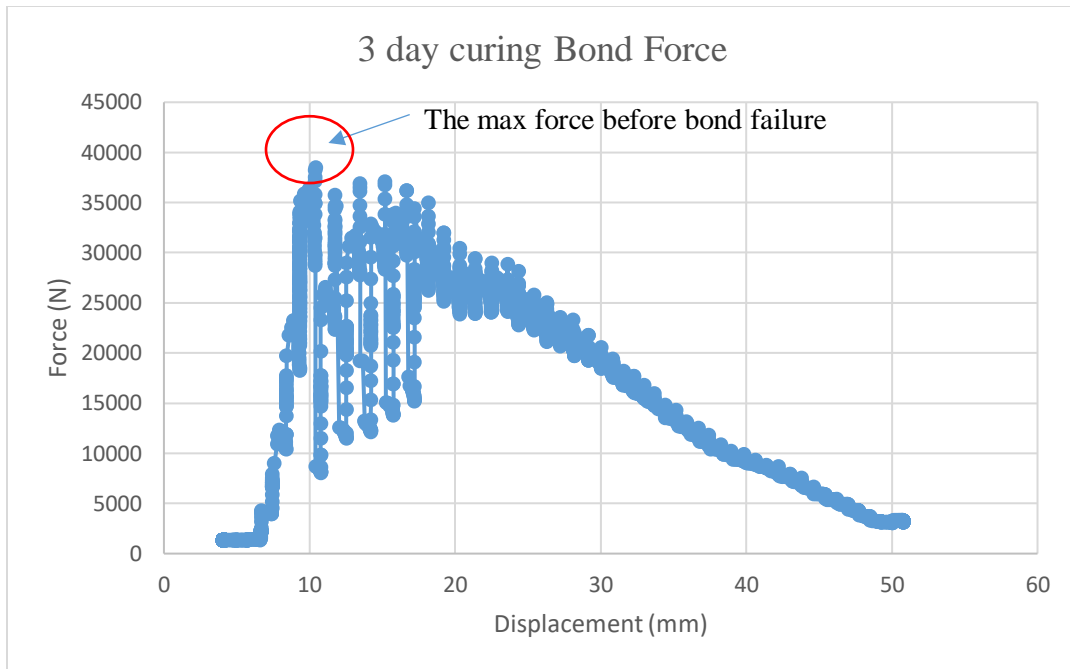


**Figure 34. Example of the Maximum Force Before Failure: 3-day bonding test**

In order to calculate stresses, equation (4) was used.

$$\sigma = \frac{F}{A} \quad (4)$$

Contact areas of cement and metal were calculated depending on the type of test would be conducted. For shear test, the contact area stays the same because shear stress is independent to the surface interaction, see the Table 4.

**Table 4. Cement and Shear Cell Contacting Area**

Cement Contact Area for pure shear experiments	
Inner Diameter (Di, mm)	54
Affected Length (Li, mm)	16.13
Contacted Area (mm <sup>2</sup> )	2735
Contacted Area (m <sup>2</sup> )	0.002735

However, contact area in bonding test is not static due to the bonding principle behind. The contact area, when calculating bonding stress, had to be adjusted as cement is replaced. Table 5 shows the method to obtain the cement- casing contact area in bonding stress calculation.

**Table 5. Cement and Bonding Cell Contacting Area**

Cement Contact Area for interfacial shear bond experiments	
Inner Diameter (Di, mm)	35.1
Affected Length (Li, mm)	50- Displacement
Contacted Area (mm <sup>2</sup> )	$35.1 * \text{PI} * (50\text{- Displacement})$
Contacted Area (m <sup>2</sup> )	$(35.1 * \text{PI} * (50\text{- Displacement})) / 10^6$

#### 4.3 Result Data

All results from Bonding, Shear, and Unconfined Compressive Strength had the same trend in changing in stress as curing day increases.

#### 4.3.1 Non-thermal effect data

**Table 6. Bonding Stress Experiment Results**

		1st attempt		2nd attempt		3rd attempt		Average
		#1	#2	#1	#2	#1	#2	
<b>Bonding Stress (MPa)</b>	<b>1day</b>	1.64	2.29	1.61	2.13	1.47	2.52	1.94
	<b>3day</b>	4.44	6.47	6.46	7.66	6.65	9.09	6.79
	<b>7day</b>	12.24	17.9	9.71	10.07	6.51	8.81	10.87
	<b>14day</b>	10.99	14.17	-	-	-	-	12.58
	<b>147day</b>	14.36	14.6	-	-	-	-	14.48

As Table 6 shows, the smallest bonding stress appeared in 1day curing was 1.47 MPa. The average bonding stress of 1day curing sample was 1.94 MPa. For 3days curing sample, the bonding stress has increased comparably drastically to 6.78 MPa of average from six samples. The increasing trend in bonding stress has been continued at 7days, 14days, and 147days of curing as 10.87 MPa, 12.58 MPa, and 14.48 MPa each. The maximum bonding stress appeared at the second sample of 147days curing days as 14.6 MPa.

**Table 7. Shear Stress Experiment Results**

		1st attempt		2nd attempt		3rd attempt		Average
		#1	#2	#1	#2	#1	#2	
<b>Shear Stress (MPa)</b>	<b>1day</b>	2.73	2.8	4.15	4.52	2.64	2.15	3.17
	<b>3day</b>	6.92	6.68	6.68	7.2	8.13	8.08	7.28

	<b>7day</b>	8.55	12.07	11.84	13.4	11.82	13.21	11.82
	<b>14day</b>	15.61	17.1	-	-	-	-	16.36
	<b>147day</b>	28.88	29.04	-	-	-	-	28.96

A similar trend has shown in shear stress test as it from bonding stress tests, see Table 7. As curing day is increased, the shear stress gets increased as well. When the curing day is the same, shear stress tends to have greater stress than bonding stress. The average shear stress at 1day curing was 3.17 MPa that is the smallest among samples, whereas the average bonding stress of 147days curing samples were the highest as 28.96 MPa.

**Table 8. Unconfined Compressive Strength Test Results**

Unconfined Compressive Strength Test Result, (MPa)							
<b>1 day 1st batch</b>	4.64	<b>3day 1st batch</b>	7.71	<b>7day 1st batch</b>	34.08	<b>14day 1st batch</b>	40.17
	5.26		-		34.09		40.83
	4.93		14.8		31.4		42.33
<b>1 day 2nd batch</b>	5.06	<b>3day 2nd batch</b>	15.04	<b>7day 2nd batch</b>	31.95	<b>147day 1st batch</b>	83.81
	5.56		13.06		31.47		55.25
	5.64		15		31.53		-
<b>1day 3rd batch</b>	4.44	<b>3day 3rd batch</b>	20.61	<b>7day 3rd batch</b>	29.09	-	-
	4.57		17.73		29.69	-	-
	5.51		20.7		34.89	-	-

1day, 3days and 7days curing samples were tested 3 times repeatedly. Each trial has 3 of API standardized 2in x2in cubes, see Table8. For 14days and 147days, one trial was tested. For second sample at 3day/1<sup>st</sup> trial and the third sample of

147days, the UCS test results presented errors, therefore the incorrect values were removed from the data summary to obtain quality results.

#### 4.3.2. Thermal effect data

In order to investigate high temperature effects to cement mechanics, high curing temperature was applied to the 3days curing sample. Same as the 3days non-thermal effect 3days curing samples, the other curing environments such as atmospheric pressure and curing water type. Elevated temperature was set to be 65°C ( $\pm 3$ ).

**Table 9. Comparison Between 3-day Curing Room Temperature and High Temperature Bonding Stress**

Bonding Stress (MPa)	1st attempt		2nd attempt		3rd attempt		Average
	#1	#2	#1	#2	#1	#2	
<b>3 day</b>	4.44	6.47	6.46	7.66	6.65	9.09	6.79
<b>3 day HT</b>	19.52	18.42	20.54	24.88	-	-	20.84

For the bonding test, 6 of non- thermal effect samples were tested, however, we could prepare only 4 samples of thermal effect samples. The result was compared with each of average values. The average result clearly showed that the samples that were cured at high temperature of 65°C $\pm 3$  showed approximately 3 times higher bonding stress in average, see Table9.

**Table 10. Comparison Between 3-day Curing Room Temperature and High Temperature Shear Stress**

Shear Stress (MPa)	1st attempt		2nd attempt		3rd attempt		Average
	#1	#2	#1	#2	#1	#2	
<b>3day</b>	6.92	6.68	6.68	7.2	8.13	8.08	7.28
<b>3day HT</b>	15.09	19.2	24.4	25.5	-	-	21.04

As shown in Table10, the average shear stress of 3day non-thermal samples was 7.28 MPa. For those cured at an elevated temperature of  $65\pm 3$  °C had higher shear stress as 21.04 MPa. There has been quite a difference in shear stress of 3 day at an elevated temperature from the first attempt and second attempt, and it is assumed that there might have been a difference (range of  $\pm 3$  °C) in temperature of curing temperature between them.

## 5. Discussions

In this chapter, we will discuss about the result from the whole experiments and analyze the data we obtained. Each test results of Shear, Bonding, and UCS will be discussed, and all of the data will be compared and analyzed together.

## 5.1 Shear Stress

**Table 11. The Average Values from All Shear Test with Curing Days**

Curing days	Shear Stress (MPa)
<b>1day</b>	3.17
<b>3day</b>	7.28
<b>7day</b>	11.82
<b>14day</b>	16.36
<b>147day</b>	28.96

Pure cement shear stress has been obtained by a lab sized experiment with the hydraulic press and customized shear cells. Portland Class H cement has been used without additives. The shear stress tended to increase as curing time increases. 147 days of curing represents a long-term investigation on cementing behavior.

The result clearly shows that the shear stresses are increased as the curing time gets longer. However, the increasing rate of shear stress is not constant as curing time change. The overall trend indicates that, the increasing rate in shear stress is the biggest at the beginning stage of curing that is between 1 day and 3 day as 2.29. The second largest increasing rate is appeared between 3 day and 7 days of curing as 1.62. However, the shear stress increasing trend tends to slow down as the samples get cured for longer days, see Table 11.

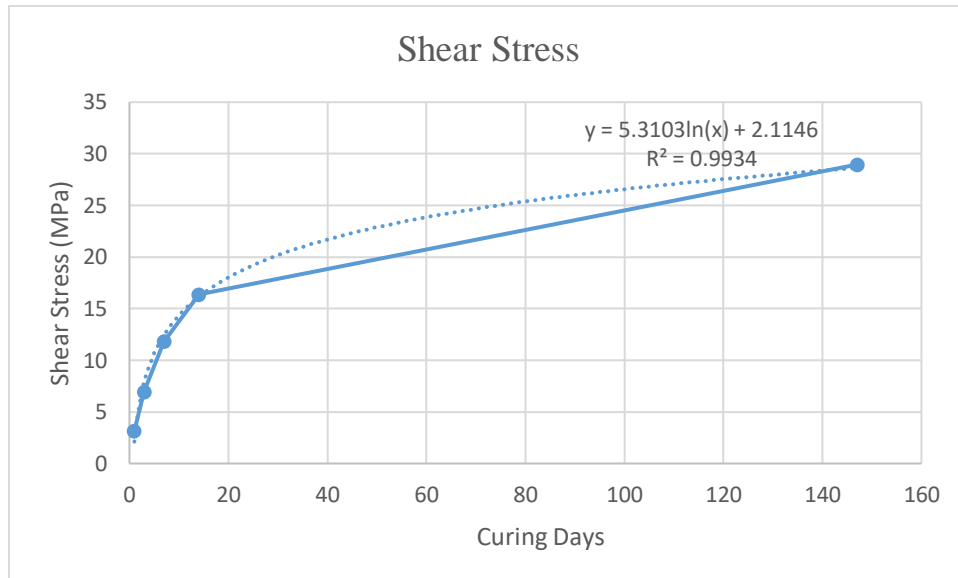


**Figure 35. Shear Stress Evolution with Curing Days**

The trend is shown in Figure35. As the curing time increases, the shear stresses also increased. At the short curing day of 1, the slop shows the biggest in a positive direction which implies that the increasement rate is the largest. Even though the increasement in shear stress keeps growing, the increasing rate represented by the slopes of each day gets stabilized as curing day gets longer towards to 147 curing day. The trend was closely relevant to the logarithmic function with coefficient determination of 0.9934.



**Figure 36. Shear Stress Samples 1day Curing (Left) and 7-day Curing (Right)**

The Figure 36 shows the tested samples for shear stress. The left picture is a sample of 1day curing time, and the right sample was cured for 7days, For the 1day curing sample, there was no cracks or debris after hydraulic load was applied and the test was completed. However, for the 7days curing sample, cracks appeared after some force was applied to the sample. With the numerical result and trend plot, we can expect that 1day curing sample was still softer compare to the 7 days curing sample. This is relevant to the result that curing day 1 sample shear stress was a lot smaller than shear stress of 7days curing sample. Hydration of cement and increasing of its UCS might be one of factors that affected to the above result. As cement hydrates as curing day increases, the cement plastic deformation would reach to failure, which means the cement is more brittle.

## 5.2 Bonding Stress

**Table 12. The Average Values from All Bonding Test with Curing Days**

<b>Curing days</b>	<b>Bonding Stress (MPa)</b>
<b>1day</b>	1.94
<b>3day</b>	6.79
<b>7day</b>	10.87
<b>14day</b>	12.58
<b>147day</b>	14.48

Similar to shear stress results, bonding stress tends to increase as time curing day increases, see Table 12. The most drastic increase was shown between curing day of 1 and 3. The increase between 14days and 147days of curing was not too big. In other words, the bonding stress tends to stabilize in a long-term curing day. As below graph shows, the bonding stress graph is also the closest to the logarithmic trend with coefficient determination of 0.8394. (Figure 37)

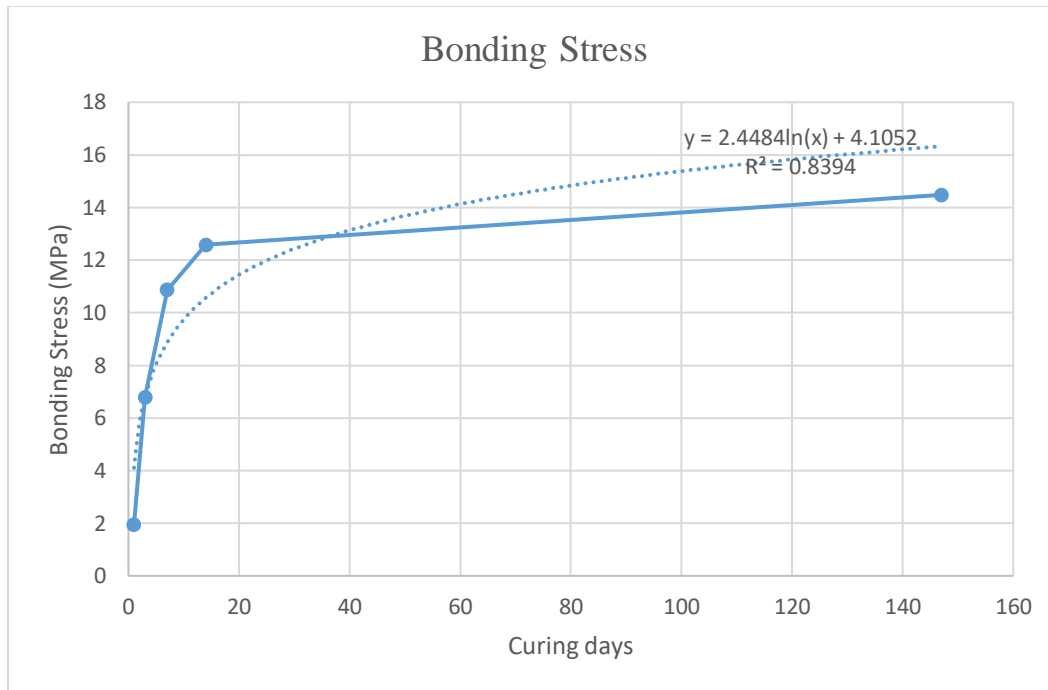


**Figure 37. Bonding Stress Evolution with Curing Days**

The slope decreases as the curing time gets longer. At the 147days of curing, the slope goes to the close to the parallel, but it shows still increasing. It is expected that the slope finally will be more stabilized with almost no increase at longer curing day than 147days.



**Figure 38. Bonding Stress 1day Curing (Left) and 7-day Curing (Right)**

Figure 38 shows the pictures of the test samples from the experiments. The left picture was a picture from 1day curing, and the right one was from 7days curing.

As it was explained at the shear stress figures in previous, the same theory would be applied to the bonding stress.

### 5.3 Unconfined Compressive Stress (UCS)

**Table 13. The Average Values from All UCS Test with Curing Days**

<b>Curing days</b>	<b>Force (N)</b>	<b>UCS(MPa)</b>
<b>1day</b>	13344.67	5.06
<b>3day</b>	43865.82	16.72
<b>7day</b>	85050	31.99
<b>14day</b>	107602.5	41.11

<b>147day</b>	176527.2	69.51
---------------	----------	-------

The smallest value in UCS was shown in 1day curing as 5.06 MPa. For 3days curing sample, the USC was more than 3times gets increased representing 16.72MPa, see table 13. Like shear and bonding stress, the increase between 1day and 3days was the biggest. It is shown in the graph in figure 39 as well. The slope decreases as the curing time gets longer.

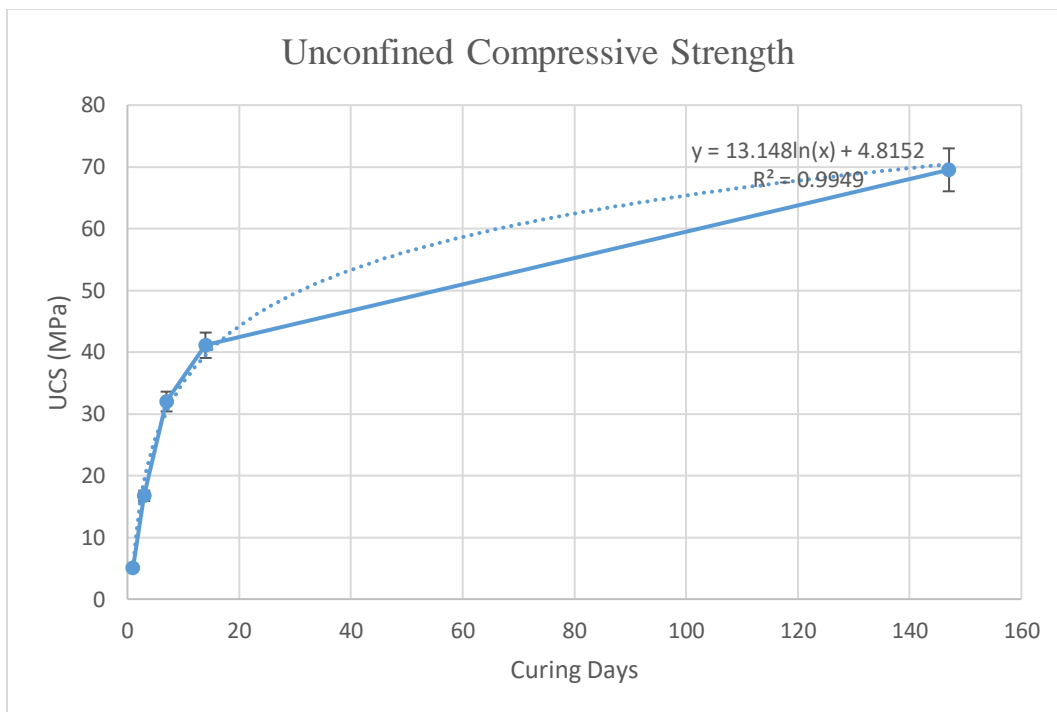


**Figure 39. UCS Evolution with Curing Days**

The UCS samples in Figure 40 are for comparison of 1day curing and 7 days curing. Higher forces were required for 7days curing samples to get the failure strength and the 7days curing tested samples showed visual cracks and they were broken into pieces. However, 1day curing samples did not show visual deformation other than light cracks.

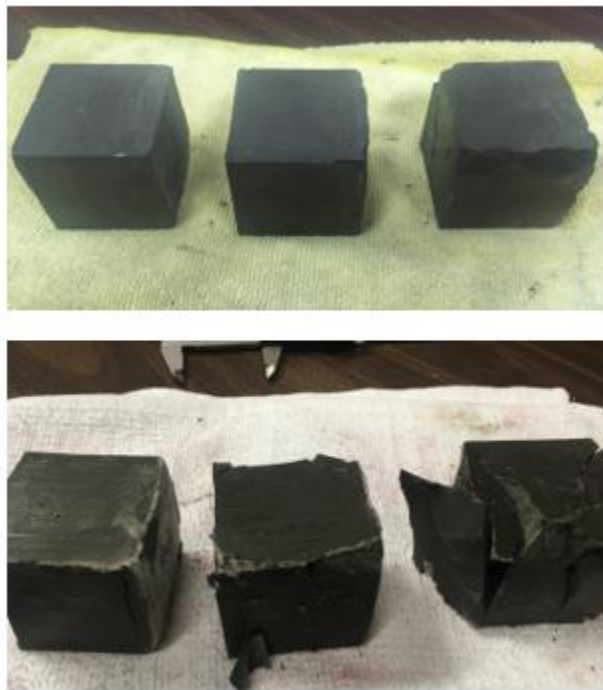


**Figure 40. Comparison of UCS Cubes After Test. 1-day Curing (Above), 7day Curing (Below)**

#### 5.4 Test Result Comparison

In the Previous sub-chapters, test results were described according to the test types.

All of the results had a common trend between stress and sample curing days showing that as curing time increases, stress also increases.

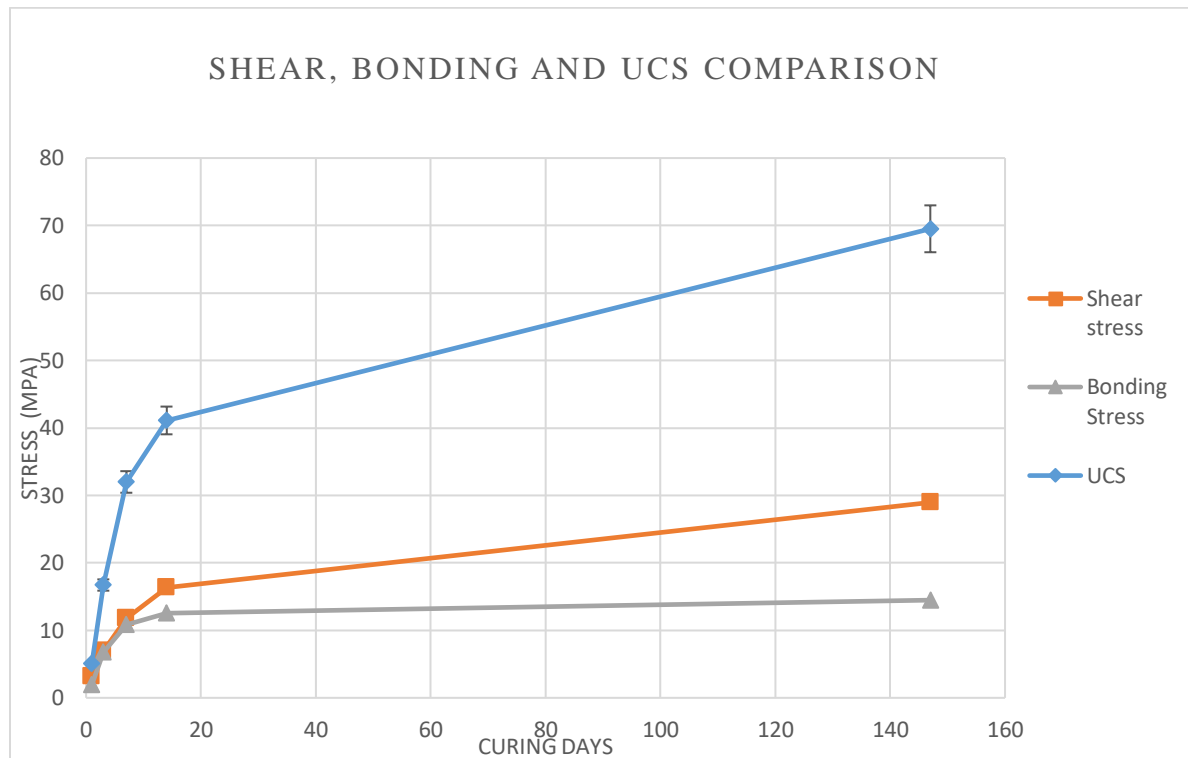


**Figure 41. Plot Comparison of Shear, Bonding, and UCS with Curing Days**

Figure 41 shows all stresses (Shear, Bonding, and UCS) result plots in one frame.

At each of same curing date, UCS always has the highest stress, and shear stress.

Bonding stress has the smallest values for all measured curing days. Also, UCS has the steepest slope at each curing day interval. Also, UCS has the biggest slope for the long-term curing day. On the contrast, the change of bonding stress was the least dramatic. For a long-term observation from 14days to 147days of curing, the change was very small compare to the others, and the graph shows almost horizontal slope. Overall, all of three stresses tend to stabilize at long term observations. In this trend, it is anticipated that there will be little changes in stress in all stresses if the curing day gets even longer than 147days.

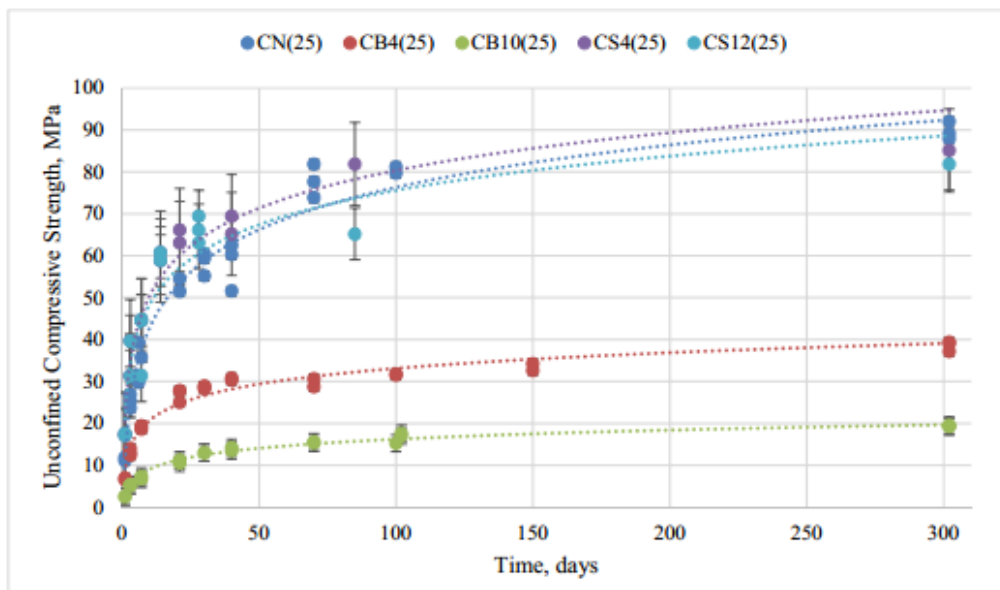


**Figure 42. Unconfined Compressive Strength Evolution with Time at 25C (Ichim, 2018)**

Figure42 shows the similar UCS evolution with time change of Class G with or without various additives according to Ichim (2016). Notation, CN represents Class

G Cement without any additives. If we see changes in UCS as curing time changes, USC of CN at curing date 147days is roughly 82MP according to the trend line developed as above. That is 12 MPa higher than Class H at 147days curing. Due to the different type of cement being used, it might not be accurate to compare UCS values of Class H cement that has been used in this thesis. However, we can see the long-term trend of Class G cement and expect how Class H would behave at long term curing days as the above graph shows. Based on the trend of UCS changes in Class G cement, it is expected that UCS of Class H cement would be also still slightly increased until certain point of long-term curing days but tend to stabilized in a long run.

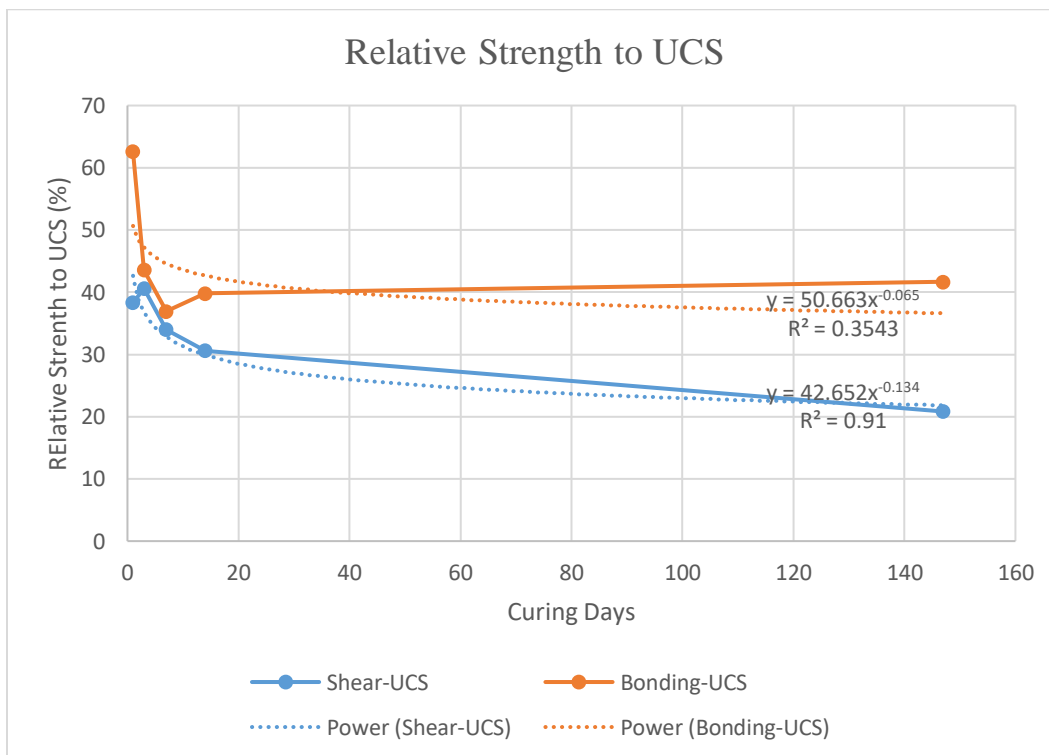


### **Figure 43. Relative Shear and Bonding Stress to UCS with Curing Time**

Figure 43 shows relative shear and bonding stress to UCS. Both of shear and bonding stress had the similar trend but with different degree. The relative shear and bonding stress to UCS were calculated as the below method.

$$\frac{\text{Bonding or Shear Stress}}{UCS} \times 100 (\%) = \text{Relative Bonding or Shear Stress to UCS} \quad (5)$$

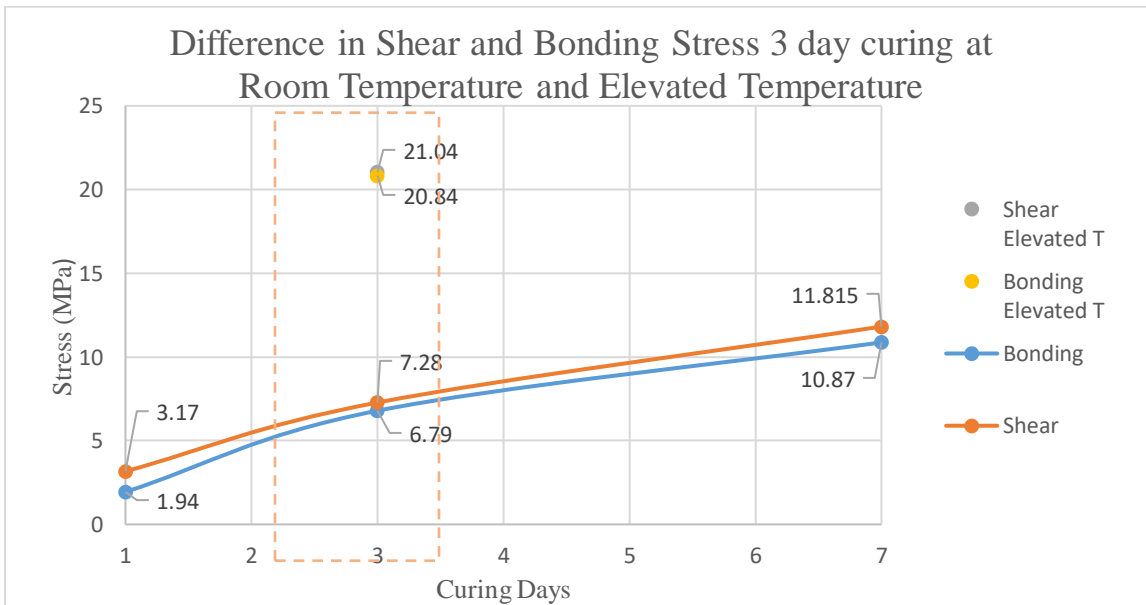
For both of shear and bonding stress, the relative strength ratio to UCS was high at a short curing time.

For bonding stress, when curing day is short, the relative strength ratio was high. This means that there is not a big difference in strength between bonding and UCS values when cement was cured for a short amount of time. However, the trend shows that as curing time becomes longer, the relative strength ratio is also getting smaller, which means there becomes bigger difference between bonding stress and UCS values. The similar trend shows in relative shear strength to UCS as well.

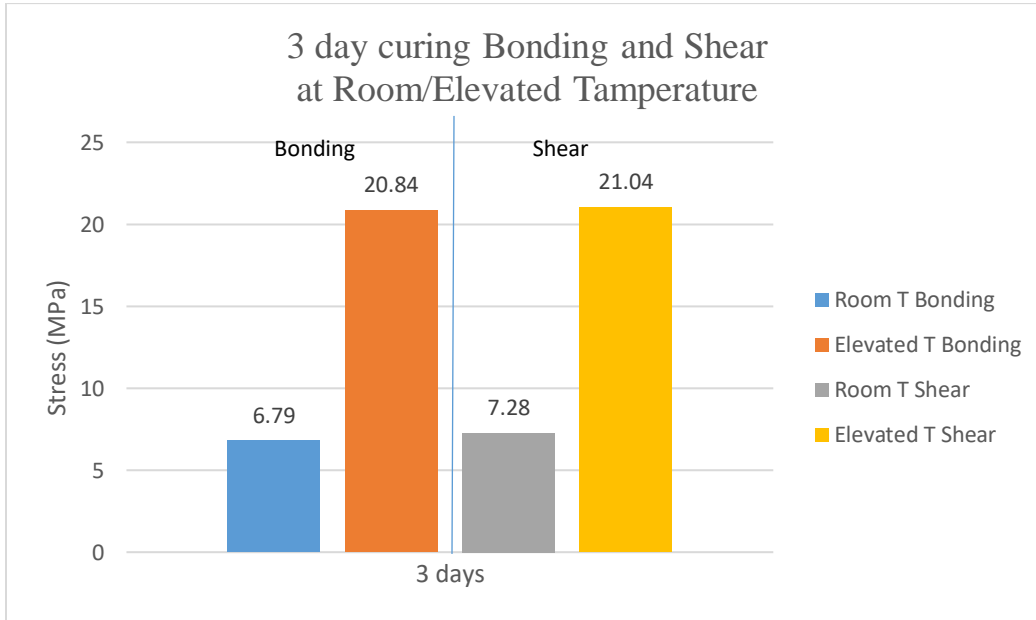
### 5.5 Comparison between 3 days non-thermal and thermal effect result

Figure44 and Figure45 show the comparison of 3 days curing time of non-thermal effect and thermal effect. Represented by “Shear Elevated T” and “Bonding Elevated T”. Elevated T (Temperature) is implying that the samples were cured at temperature of  $65^{\circ}\text{C}\pm 3$ . Non-thermal effect samples were cured at room temperature of  $22^{\circ}\text{C}\pm 2$ .

From Figure 44 and 45, it is shown that bonding and shear strength samples that were cured in an elevated temperature required higher force to reach failure points. This implies that, at a higher temperature environment, cement H become harden faster. Both in room temperature and high temperature, shear stress tends to have higher values compare to bonding stress.



**Figure 44. 3-day curing Thermal effected and Non-thermal effected Shear and Bonding Stress Comparison 1**



**Figure 45. 3-day curing Thermal effected and Non-thermal effected Shear and Bonding Stress Comparison 2**

### 5.6. Correlations of UCS Vs. Shear / UCS Vs. Bonding

Based on obtained results from the experiment, the correlations between Bonding stress and UCS/Shear stress and UCS have been constructed as Figure 46 and Figure 47.

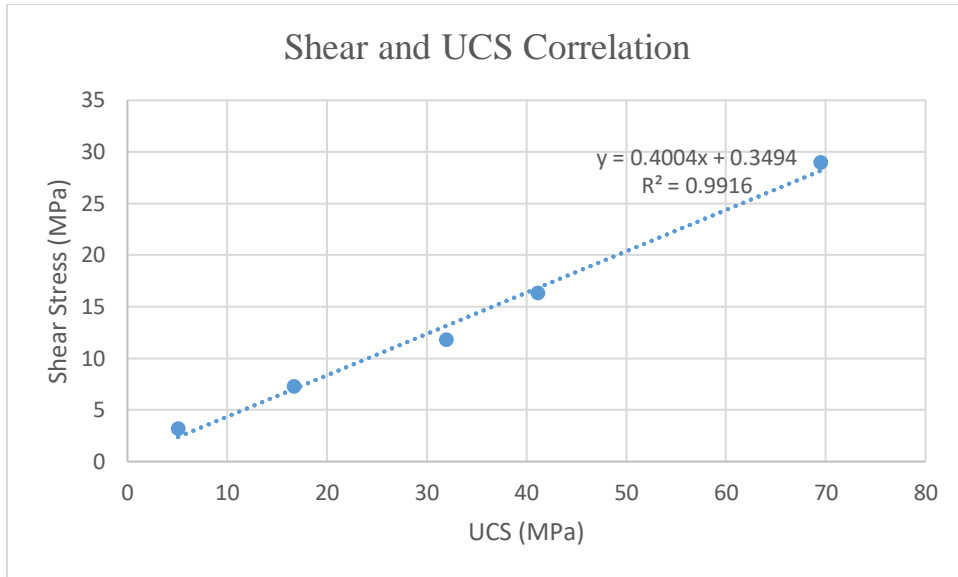


**Figure 46. Class H Cement Shear and UCS Correlation**

Figure 46 shows the plot of correlation between Shear stress and UCS. The correlation is described the best as the first order linear equation.

$$\text{Shear Stress} = 0.4004 \text{ UCS} + 0.3493 \quad (6)$$

With a coefficient determination of 0.9916.

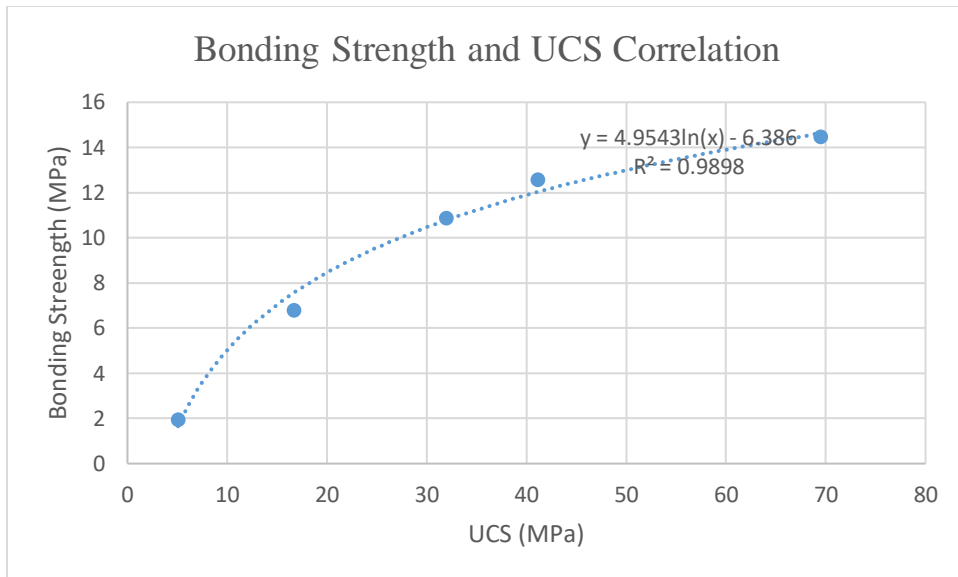


**Figure 47. Class H Cement Bonding and UCS Correlation**

Whereas the correlation between shear stress and UCS is constructed as a linear line, a trend of the correlation between bonding and UCS is shown as a logarithmic equation of

$$\text{Bonding Stress} = 4.9543 \ln(\text{UCS}) - 6.386 \quad (7)$$

with a coefficient determination of 0.9898.

Both shear stress and bonding stress tend to increase as UCS gets greater, however increasement of bonding stress tends to slow down at a higher UCS.

## 6. Conclusions and Recommendations

The obtained data is in line with previously published data by Teodoriu et al (2018), Salehi et al (2016), Lavrov and Torsaer (2016), and Zhao et al (2015) and it is shown in table 14. Nevertheless, only the interfacial debonding data could be compared since no previous work has proposed a pure shear test comparable with the ones performed in this thesis. It must be noted that commonly, interfacial bonding strength is evaluated at 24 hours only.

**Table 14. Comparison of literature values with obtained data**

<b>Author</b>	<b>Salehi et al. 2016</b>	<b>Lavrov and Torsaer 2016</b>	<b>Zhao et al. 2015</b>	<b>Zhao et al. 2015</b>	<b>Teodoriu et al 2018</b>
<b>Comment</b>	After 24 h	-	-	Added sand to casing	After 24 hours
<b>Shear Bonding Strength (PSI)</b>	139.6	14.5 to 145	14.5 to 362.5	-	68
<b>Shear Bonding Strength (MPa)</b>	0.96	0.1 to 1.0	1.0 to 2.5	2.5 to 7.5	0.47

The novelty of this work is customized cell designs and the time span in which tests were conducted. To better understand the cement behavior, a new testing procedure was designed. Class H neat cement was used for the entire experiment and no

additives were added. Samples for Shear strength, Bonding strength, and UCS were mixed and cured at room temperature of  $22^{\circ}\text{C}\pm 2$ . Also, 3 days of high temperature ( $65\pm 3^{\circ}\text{C}$ ) cured samples were tested for a purpose of comparison to non-thermal effect of 3 days cured samples of shear and bonding strength. Pressure has been kept constant throughout the entire experiments. The results were obtained with variation in curing time and temperature.

The test result has shown that the shear stress is typically higher than the cement bonding stress at the same curing day, which confirms that under certain downhole conditions, the casing and cement would go through de-bonding process first and then fail in shear in the vicinity of the couplings with a square external shoulder.

At room temperature of  $22^{\circ}\text{C}\pm 2$ ,

- Shear stress was the lowest at 1day curing as 3.17 MPa and the highest at 147day curing as 28.96 MPa.
- Bonding stress was the lowest at 1day curing as 1.94 MPa and the highest at 147day curing as 14.48MPa.
- UCS was the lowest at 1day curing as 5.06MPa and the highest at 147day as 69.51MPa.
- The increasing rate tend to be stable for short term curing time. ( Graph trend increases in positive )
- The increasing rate becomes smaller as curing time gets longer in all of shear stress, bonding stress, and UCS. (Graph trend gets stabilized)

- For the same curing day comparison, shear stress is higher than bonding stress for all observed curing days of 1,3,7,14 and 147.
- The difference between shear and bonding stress gets larger as curing time gets longer.

At elevated temperature of  $65\pm 3^{\circ}\text{C}$  for 3 curing days,

- Both bonding and shear stress were higher than sample cured for the same days at room temperature.
- Bonding stress at high temperature appeared as 20.84 MPa and it was almost as 3 times as higher than it was at room temperature.
- Shear stress at high temperature appeared as 21.04 MPa and it was also as almost 3 times (accurately 2.89) as higher than it was at room temperature.
- Moreover, we observed that shear stress has a linear dependency of UCS. On the other side the bonding stress seem to show a logarithmic behavior. These findings are novel and allow scientists to easily access cement mechanical properties when only UCS is known.

It is recommended that for the future work, various curing temperature can be added with pressure effects considering together with additional cement formulations and different simulated coupling geometry. For more accurate observation in changing of cement mechanical behaviors, not only for long term curing days but short-term curing days can be added.

Also, different casing material could be suggested to observe bonding stress between cement and the hardware.

Furthermore, the plasticity of the cement should be investigated in order to understand if shear bonding improvements versus shear strength are sustainable.

## REFERENCES

Santos, O.L. 2017. An Overview of Deepwater Well Integrity Developments After the Blowout of Macondo. Presented at the SPE Latin America and Caribbean Petroleum Engineering Conference, Buenos Aires, Argentina, 18—19 May.

Rowmanowski, N., Ichim, A., and Teodoriu, C. 2017. Investigation on Oilwell Cement Response to Ultrasonic Measurements in Presence of Additives. Presented at the ASME 2017 36th International Conference on Ocean, Offshore and Arctic Engineering, Trondheim, Norway, 25—30 June.

Teodoriu, C., Yi, M., Ichim, A. et al. 2018. A Novel View of Cement Failure with Application to Geothermal Well Construction. Presented at the Stanford Geothermal Workshop, Stanford, California, 12—14 February.

Salehi, S., Ezeakacha, P.C., and Khattak, J.M. 2017. Geopolymer Cement: How Can You Plug and Abandon a Well with New Class of Cheap Efficient Sealing Materials. Presented at the Oklahoma City Oil and Gas Symposium, Oklahoma City, Oklahoma, 27—31 March.

Alber, M. and Ehringhausen, N. 2017. Petrophysical Properties of Casing Cement While Curing. Presented at the ISRM European Rock Mechanics Symposium, Ostrava, Czech Republic, 20—22 June.

Kosinowski, C. and Teodoriu, C. 2012. Study of Class G Cement Fatigue using Experimental Investigations. Presented at the SPE/EAGE European Unconventional Resources Conference and Exhibition, Vienna, Austria, 20—22 March.

Ichim, A. and Teodoriu, C. 2017. Development of a Cement Repository to Improve the Understanding of Well Integrity Behavior with Time. Presented at the SPE

Oklahoma City Oil and Gas Symposium, Oklahoma City, Oklahoma, 27—31 March.

Salehi, S., Khattak, M.J., and Ali, N. 2016. Development of Geopolymer-based Cement Slurries with Enhanced Thickening Time, Compressive and Shear Bond Strength and Durability. Presented at the IADC/SPE Drilling Conference and Exhibition, Fort Worth, Texas, 1—3 March.

Philippacopoulos, J.A. and Berndt, L.M. 2002. Geomechanics. In Structural Analysis of Geothermal Well Cements, sixth edition, 657—676.

Albarwary, I. and Haido, H.J. 2013. Bond Strength of Concrete With the Reinforcement Bars Polluted With Oil. Presented at the European Scientific Journal.

Evans, G. and Carter, G.L. 1962. Bonding Studies of Cementing Compositions to Pipe and Formations. Presented at the Drilling Production Practice, New York, New York, 1 January.

Pochman, R. 2016. Bond Strength Testing of Wellbore Material Composites. Montan University.

Knab, L.I. and Spring, C.B. 1988. Evaluation of Test Methods for Measuring the Bond Strength of Portland Cement Based Repair Materials to Concrete. U.S. Department of Commerce National Bureau of Standards-Center for Building Technology Building Materials Division.

Ytrehus, J.D. and Stroisz, A. 2018. Casing Removal Tests in Laboratory Setup. Presented at the ASME, Madrid, Spain, 17—22 June.

Lummer, N.R., Block, R., and Yadigarov, Y. 2017. Specialty Customized System for Cementing Glass Reinforced Epoxy GRE Casing-Development and Field Trials in a Geothermal Project. Presented at the SPE/IADC Drilling Conference and Exhibition, Hague, Netherlands, 14—16 March.

McCabe, A.C. 1989. Well Vertical Movement On Platform Wells. Presented at the Offshore Europe 89, Aberdeen, United Kingdom, 5—8 September.

Teodoriu, C., Kosinowski, C., and Amani, M. 2013. Wellbore Integrity And Cement Failure at HPHT. Presented at the International Journal of Engineering and Applied Science.

Liu, X. 2014. Zonal Isolation Improvement Through Enhanced Cement-Shale Bonding. Austin, Texas: The University of Texas at Austin.

EIA, N. U.S. Energy Information Administration. Annual Energy Outlook 2018, [www.eia.gov/aeo](http://www.eia.gov/aeo)(accessed 06 February 2018).

Suryakanta, N. CivilBlog. HOW TO DETERMINE OF BOND STRENGTH BETWEEN STEEL CONCRETE?, [www.civilblog.org](http://www.civilblog.org)(accessed 22 June 2015).

Ichim, A. 2017. Experimental Determination Of Oilfield Cement Properties And Their Influence on Well Integrity. Norman, Oklahoma: The University of Oklahoma.

Saleh, F. 2018. Investigation Of Oil Well Cement Mixing Experimental Studies And Implications For Mixing Energy Theory. Norman, Oklahoma: The University of Oklahoma.

Saleh, F. and Teodoriu, C. 2016. The Mechanism Of Mixing and Mixing Energy for Oil and Gas Wells Cement Slurries: A Literature Review and Benchmarking of the Finding Journal of Natural Gas Science and Engineering.

Rystad Energy. Outlook for the Global Drilling and Well Services Market , [www.rystadenergy.com](http://www.rystadenergy.com)(accessed 14 November 2018).

Shahriar, A. 2011. Investigation on Rheology of Oil Well Cement Slurries. Ontario, Canada: The University of Western Ontario.

Reddy, B.R., Santra, A.K., and McMechan, D.E. 2007. Cement Mechanical Property Measurement Under Wellbore Conditions. Presented at the Drilling and Completion.

Vignes, B. and Tønning, S.A. 2008. Injection Wells with Integrity Challenges on the NCS. Presented at the Abu Dhabi International Petroleum Exhibition and Conference, Abu Dhabi, United Arab Emirates, 3—6 November.

Nath, F., Kimanzi, R.J., Mokhtari, M. Salehi, S. et al. 2018. A novel Method to Investigate Cement-Casing Bonding Using Digital Image Correlation. Journal of Petroleum Technology.

Haddad, R. H., Al-Rousan, R., Almasry, A. “Bond-slip behavior between carbon fiber reinforced polymer sheets and heat-damaged concrete.”. Composites: Part B: Engineering, 45(1), pp. 1049–1060.

2013. <https://doi.org/10.1016/j.compositesb.2012.09.010>

Smith, D.K. 1974. Cements and Cementing. In DPM.

Hole, H. M. 2008. Geothermal Well Cementing. Vol. Workshop 28. Dubrovnik: Petroleum Engineering Summer School

Nelson, E., and Guillot, D. 2006. Oilwell Cementing, Second edition, Schlumberger publications

Polkowski, G. 1987. Correlation of Oilwell Cement Performance With Cement Characteristics. Presented at the 62nd Annual Technical Conference and Exhibition of Society of Petroleum Engineer, Dallas, Texas, 27—30 September.